Dynamical Characteristics of Soil-Structure Cross-Interaction System, I

KOBORI, Takuji; MINAI, Ryoichiro; KUSAKABE, Kaoru

Bull. Disas. Prev. Res. Inst., Kyoto Univ., Vol. 22, Part 2, No. 204, February, 1973

Dynamical Characteristics of Soil-Structure Cross-Interaction System, I

By Takuji KOBORI, Ryoichiro MINAI and Kaoru KUSAKABE

(Received February 15, 1973)

Abstract

This paper deals with the cross-interaction problem which means the dynamic interaction problem among the multi-structure system through soilground. The model of such a soil-structure system is supposed to be a multi-mass or multi-spring-mass system on a visco-elastic stratum over the rigid bed rock. Two types of excitation are considered; force excitation at one of masses or basement masses and the other is the uniform displacement excitation at the free surface or the soil-rock interface of the stratum. All the dynamical characteristics of the soil-structure system are discussed in the form of dimensionless transfer functions.

In order to formulate such cross-interaction problem, the dynamical ground compliance matrix associated with multi-foundation system on the Voigt type visco-elastic stratum, which is a complex-valued symmetric matrix representing the set of displacement transfer functions of foundation areas to the force excitation on each foundation area, the displacement transfer function at the free surface of the visco-elastic stratum to the uniform displacement excitation at the soil-rock interface, and the displacement and force transfer functions of an elastic shear type spring-mass system to the displacement excitation at the basement, are determined. And then, the transfer functions of the horizontal displacements of the soil-structure cross-interaction system subjected to the two types of excitation in the same horizontal direction are expressed in terms of the above-mentioned basic transfer functions associated with the visco-elastic stratum and the elastic structures.

The numerical analyses are carried out in the cases of identical two and seven-mass systems and of identical and different two-spring-mass systems, all of which have the same square foundations on the visco-elastic stratum, and also in the cases of a single mass and a single spring-mass system for the sake of comparison. From the amplitude characteristics of the dimensionless transfer functions of the soil-structure system, the following remarks are obtained:

(1) The effects of the cross-interaction on the dynamical characteristics of the soil-structure system are different considerably depending on whether the lowest natural frequency due to the structure-subsoil interaction is smaller or not than the fundamental natural frequency of the stratum. If the lowest natural frequency is in the lower frequency range, the amplitude characteristics are sharp and the cross-interaction effect appears in the neighbourbood of the natural frequency. If contrary, the amplitude characteristics are broadened and the cross-interaction effect covers the wide frequency range containing the lower natural frequencies of the soil-structure system.

(2) The cross-interaction effects depend on the type of excitation, the number of structures and the dynamical characteristics of structures. In the case of the identical two structures subjected to the uniform displacement excitation at the free surface of the stratum, the cross-interaction effect is smaller as compared with the case of the force excitation at one of the two structures. In the case of different structures, however, the effects are rather large for the displacement excitation than for the force excitation.

(3) As the number of structures increases, the cross-interaction becomes complicated and the maximum peak value of the amplitude characteristics in the case of the uniform displacement excitation becomes large because of the increase of the transmitted energy as well as the dispersion of the peak values.

(4) The amplitude characteristics of a structure are considerably influenced by the cross-interaction in the vicinity of the fundamental natural frequency of the adjacent structures. The cross-interaction effect becomes remarkable as the fundamental frequencies of the structures are close to each other and their masses are large as compared with the foundation area.

Nomenclatures

λ, μ =Lame's elastic constants

λ', μ' =viscosity constants corresponding to Lame's elastic constants

ν =Poisson's ratio

ρ =density of stratum

B_0 =reference value of length

$\boldsymbol{U}=\{U, V, W\}$ =displacement vector

$\boldsymbol{x}=\{x, y, z\}=\left\{\frac{X}{B_0}, \frac{Y}{B_0}, \frac{Z}{B_0}\right\}$ =dimensionless Cartesian coordinates

$\{x_l, y_l, 0\}$ =dimensionless coordinates of the center of the l-th area

$V_p=\sqrt{(\lambda+2\mu)/\rho}$ =P-wave velocity

$V_s=\sqrt{\mu/\rho}$ =S-wave velocity

$\eta_s=\frac{V_s}{B_0}\frac{\mu'}{\mu}$ =dimensionless viscosity coefficient corresponding to S-wave

$\eta_p=\frac{V_s}{B_0}\frac{\lambda'+2\mu'}{\lambda+2\mu}=n^2\eta_s\left(2+\frac{\lambda'}{\mu'}\right)$ =dimensionless viscosity coefficient corresponding to P-wave

$n=V_s/V_p$ =velocity ratio of S-wave to P-wave

τ_{zx}, τ_{yz}, σ_z =tangential and normal stresses

P_x, P_z =amplitude of exciting force parallel to the X- and Z-axis of the l-th area, respectively

M_y =amplitude of exciting moment about the principal axis parallel to the Y-axis of the l-th area

$b_i=B_i/B_0$, $c_i=C_i/B_0$ =dimensionless half length of each side of the i-th rectangular foundation

$h=H/B_0$ =dimensionless thickness of stratum

$a_0=\omega B_0/V_s$ =dimensionless frequency in which ω is frequency

$\tau=tV_s/B_0$ =dimensionless time in which t is time

$x=|\boldsymbol{x}_k-\boldsymbol{x}_l|$ =dimensionless distance between the k-th and l-th areas

J^{Xk}_{Zl}, J^{Yk}_{Zl}, J^{Zk}_{Zl} =ground compliances for translation parallel to the X-, Y- and Z-axis of the k-th foundation due to vertical excitation at the l-th area, respectively

J^{ZXk}_{Zl}, J^{YZk}_{Zl} =ground compliances for rotation about the principal axis parallel to the Y- and X-axis of the k-th area due to the vertical excitation of the l-th area, respectively

J^{Xk}_{Xl}, J^{Yk}_{Xl}, J^{Zk}_{Xl} =ground compliances for translation parallel to the X-, Y- and Z-axis of the k-th area due to horizontal excitation in the X-direction of the l-th area, respectively

J^{ZXk}_{Xl}, J^{YZk}_{Xl} =ground compliances for rotation about the principal axis parallel to the Y- and X-axis of the k-th area due to the horizontal excitation in the X-direction of the l-th area, respectively

$J_{ZX^l}^{Xk}$, $J_{ZX^l}^{Yk}$, $J_{ZX^l}^{Zk}$ =ground compliances for the translation parallel to the X-, Y- and Z-axis of the k-th area due to rotational excitation about the

principal axis parallel to the Y-axis of the l-th area, respectively

J^{zxk}_{zxl}, J^{yzk}_{zxl} =ground compliances for rotation about the principal axis parallel to Y- and X-axis of the k-th area due to rotational excitation about the principal axis parallel to the Y-axis of the l-th area, respectively

$|J|$ =amplitude characteristics of J

$m^j_i=\dfrac{M^j_i}{B^3_0\rho}$ =the j-th dimensionless mass (the j-th mass ratio) of the i-th structural system

$m^0_i=\dfrac{M^0_i}{B^3_0\rho}$ =dimensionless basement mass (basement mass ratio) of the i-th structural system

$k^j_i=\dfrac{K^j_i}{B_0\mu}$ =the j-th dimensionless shear stiffness of the i-th structural system

$c^j_i=\dfrac{C^j_i}{B^2_0\sqrt{\rho\mu}}$ =the j-th dimensionless damping coefficient of the i-th structural system

$\hat{k}^j_i=k^j_i+ja_0c^j_i$ =the j-th dimensionless complex shear stiffness of the i-th structural system

u^0_i, u^j_i =dimensionless displacements of the basement and the j-th level of the i-th structural system

ζ_i =critical damping ratio of the fundamental mode of the i-th structural system

λ_i =fundamental natural frequency ratio of the i-th structural system to stratum

$r^0_i=\dfrac{R^0_i}{B^2_0\mu}$ =dimensionless force to stratum of the i-th structural system

J^k_l =ground compliance for horizontal translation of the k-th area due to horizontal excitation at the l-th area

L =total number of structural systems

N_i+1 =degrees of freedom of the i-th structural system including the basement mass

m_i =the i-th dimensionless mass (the i-th mass ratio) of the multi-mass system

$S_i=\{m^0_i, m^1_i, \lambda_i\}$ =type of the i-th structural system of the multi-spring-mass system

${}_iG^0_l$, ${}_iG^j_l$ =displacement transfer functions of the basement and of the j-th level of the i-th structural system due to force excitation at the basement mass of the l-th structural system, respectively

${}_iG^0_S$, ${}_iG^j_S$ =displacement transfer functions of the basement and of the j-th level of the i-th structural system to the uniform displacement excitation at the free surface of stratum

${}_iG^j_0$ =displacement transfer function of the j-th level of the i-th structural system to displacement excitation at the basement mass

${}_iG^0_B$, ${}_iG^j_B$ =displacement transfer functions of the basement and of the j-th level of the i-th structural system to the uniform displacement excitation at soil-rock interface

G^s_B =displacement transfer function of the surface of stratum to displacement excitation at soil-rock interface

$|G|$ =amplitude characteristics of G

1. Introduction

It has been well-known that the earthquake response characteristics of structures are considerably affected by the properties of the soil-ground through the interaction between a structure and its surrounding sub-soil[1)-14)] as well as the filtering action of the soil layers over the bed rock[19),20)]. As in the big cities in Japan, however, the building structures are built closely to each other over the soft soil deposit. In these circumstances, the dynamic interaction among building structures must occur through the radiation energy emitted from a vibrating structure to other structures. Hence the dynamical characteristics as well as the earthquake response characteristics of a structure are unable to be independent of those of the adjacent structures. It is evident that the effect of dynamical characteristics of a structure on those of the adjacent structures is remarkable when the mass of the structure becomes large as compared with the mass of the adjacent structure and the distance between the structures becomes short. However, if the structures have masses of comparative order and their dynamical characteristics are not so different each other, the interaction between structures through soil ground may be strong, and hence the dynamical characteristics of both structures should be considerably different from those in the case of the single structure on the same soil ground[15)-18)].

In this paper, the above-mentioned interactions are called the "cross-interaction" among the structures though soil ground, and the objective of this paper is indeed to find the effects of such cross-interaction on the dynamical characteristics of the multi-structure system on a visco-elastic soil ground. As the models to study the cross-interaction problem, the multi-mass system or the multi-spring-mass system which are along a line on the surface of the Voigt type visco-elastic stratum over the rigid bed rock are considered. Then, supposing the two types of excitation one of which is the force excitation at one of the multi-mass system or one of the basement masses of the multi-spring-mass system and the other is the uniform displacement excitation at the surface or soil-rock interface of the stratum, the dynamical characteristics are discussed in the form of dimensionless transfer functions of displacements of the soil-structure system to each type of excitation.

At first, as the basic transfer function necessary to analyze such a interaction problem, the dynamical ground compliances of a rectangular foundation on the Voigt type visco-elastic stratum over the rigid bed rock are formulated by using the averaging procedure weighted by the stress distribution in the foundation area[1)] so that the reciprocal theorem is valid for the ground compliances of the multi-foundation system. Next, by making use of the displacement and force transfer functions of the multi-structure system to the displacement excitations at their basements as well as the above-mentioned ground compliances, the formulation of the cross-interaction problem of the soil-structure system is developed in the matrix forms, particularly paying attention to the horizontal components of both the output response and input excitation. Then, the effects of the cross-interaction of the identical two-mass or seven-mass system and the identical or different two-spring-mass system, all of which have the identical square foundations along a line on the surface of the Voigt type visco-elastic stratum over the rigid bed rock, are discussed based upon the amplitude characteristics of the dimensionless transfer functions in comparison to those of the single mass and the single spring-mass systems on the same stratum.

2. Dynamical Ground Compliances of Rectangular Foundations on a Visco-Elastic Stratum

In order to obtain the basic dynamical characteristics of a soil-multi-foundation system, the analytical expressions of the dynamical ground compliances of a rectangular foundation on the surface of the Voigt type visco-elastic stratum on the rigid bed rock are developed for the three types of distributed harmonic force excitations which are the vertical and horizontal excitations and the rotational excitation about a principal axis of rectangular area. The ground compliance of a rectangular foundation is defined as the dimensionless force-displacement transfer function which means the complex amplitude ratio of the average Fourier transformed displacement weighted by the stress distribution in a rectangular area on the surface of the ground to the total transformed force applied to another rectangular area on the same surface.

2.1. Analytical Expressions of Ground Compliance

For the homogeneous isotropic Voigt solid, the displacement vector $\boldsymbol{U}$ satisfies the following vector equation:

$$\left[(\lambda+\mu)+(\lambda'+\mu')\frac{\partial}{\partial t}\right]\nabla(\nabla\cdot\boldsymbol{U})+\left(\mu+\mu'\frac{\partial}{\partial t}\right)(\nabla\cdot\nabla)\boldsymbol{U}=\rho\frac{\partial^2}{\partial t^2}\boldsymbol{U} \tag{2.1}$$

in which t is time, ∇ the gradiant operator with respect to spatial coordinates, λ and μ are Lame's elastic constants, λ' and μ' the corresponding viscosity constants, and ρ is density of the solid. By taking the right-hand Cartesian coordinates system (X, Y, Z) with the X–Y plane on the surface of the stratum and the Z-axis in the downward direction, the solution $\boldsymbol{U}=\{U, V, W\}$ of Eq. (2.1) is obtained in the following form through the triple Fourier transform with respect to X, Y and t:

$$\begin{aligned}\{U, V, W\}&=\mathscr{F}^{-3}[\{\bar{U}(\beta, \gamma, \omega), \bar{V}(\beta, \gamma, \omega), \bar{W}(\beta, \gamma, \omega)\}]\\&=\mathscr{F}^{-3}\Big[\{-j\beta A_1, -j\gamma A_1, -\alpha_1 A_2\}\frac{1+j\omega d_p}{\eta^2}\sinh\alpha_1 Z\\&\quad+\{-j\beta A_2, -j\gamma A_2, -\alpha_1 A_1\}\frac{1+j\omega d_p}{\eta^2}\cosh\alpha_1 Z\\&\quad+\Big\{B_1, C_1, -\frac{j}{\alpha_2}(\beta B_2+\gamma C_2)\Big\}\sinh\alpha_2 Z\\&\quad+\Big\{B_2, C_2, -\frac{j}{\alpha_2}(\beta B_1+\gamma C_1)\Big\}\cosh\alpha_2 Z\Big]\end{aligned} \tag{2.2}$$

in which

$$\alpha_1^2=\beta^2+\gamma^2-\frac{\eta^2}{1+j\omega d_p},\qquad \alpha_2^2=\beta^2+\gamma^2-\frac{\kappa^2}{1+j\omega d_s}$$

$$\eta^2=\frac{\omega^2}{V_p^2},\qquad \kappa^2=\frac{\omega^2}{V_s^2},\qquad j=\sqrt{-1}$$

$$V_p=\sqrt{\frac{\lambda+2\mu}{\rho}},\qquad V_s=\sqrt{\frac{\mu}{\rho}}$$

$$d_p=\frac{\lambda'+2\mu'}{\lambda+2\mu}\qquad d_s=\frac{\mu'}{\mu} \tag{2.3}$$

where ω is frequency and β, γ denote the wave number corresponding to the X- and Y- direction, V_p, V_s are P- and S-wave velocity and d_p, d_s are the corresponding viscosity coefficients. In Eq. (2.2), $\{\bar{U}(\beta,\gamma,\omega),\ \bar{V}(\beta,\gamma,\omega),\ \bar{W}(\beta,\gamma,\omega)\}$ means the triple Fourier transform of $\{U, V, W\}$, and the triple inverse operator $\mathscr{F}^{-3}$ is defined as

$$\mathscr{F}^{-3}[\{\bar{U}(\beta,\gamma,\omega),\ \bar{V}(\beta,\gamma,\omega),\ \bar{W}(\beta,\gamma,\omega)\}]=\{U, V, W\}$$
$$=\left(\frac{1}{2\pi}\right)^{3/2}\int_{-\infty}^{\infty}\int_{-\infty}^{\infty}\int_{-\infty}^{\infty}\{\bar{U}(\beta,\gamma,\omega),\ \bar{V}(\beta,\gamma,\omega),\ \bar{W}(\beta,\gamma,\omega)\}e^{i(X\beta+Y\gamma+t\omega)}d\beta d\gamma d\omega \tag{2.4}$$

where – represent the triple Fourier transform with respect to time t and spatial coordinates, X and Y. Also, A_1, A_2, B_1, B_2, C_1 and C_2 in Eq. (2.2) are the arbitrary functions of the parameters β, γ and ω, which are to be determined from the boundary conditions on the surface ($Z=0$) and the interface between the stratum and the bed rock ($Z=H$).

With the aid of Eqs. (2.2) and (2.4), the stress components $\{\tau_{ZX}, \tau_{YZ}, \sigma_Z\}$ at $Z=0$ are expressed respectively as follows;

$$\tau_{ZX}|_{Z=0}=-\mu\mathscr{F}^{-3}\left[(1+j\omega d_s)\left(2j\beta\alpha_1\frac{1+j\omega d_p}{\eta^2}A_1-\frac{\beta^2+\alpha_2^2}{\alpha_2}B_1-\frac{\beta\gamma}{\alpha_2}C_1\right)\right] \tag{2.5}$$

$$\tau_{YZ}|_{Z=0}=-\mu\mathscr{F}^{-3}\left[(1+j\omega d_s)\left(2j\gamma\alpha_1\frac{1+j\omega d_p}{\eta^2}A_1-\frac{\beta\gamma}{\alpha_2}B_1-\frac{\gamma^2+\alpha_2^2}{\alpha_2}C_1\right)\right] \tag{2.6}$$

$$\sigma_Z|_{Z=0}=-\mu\mathscr{F}^{-3}\left[(1+j\omega d_s)\left\{(\alpha_2^2+\beta^2+\gamma^2)\frac{1+j\omega d_p}{\eta^2}A_2+2j\beta B_2+2j\gamma C_2\right\}\right] \tag{2.7}$$

Referring to Fig. 1, the two rectangular areas, both of which have the sides parallel to the X- and Y-axis, are considered and the ground compliance associated with the

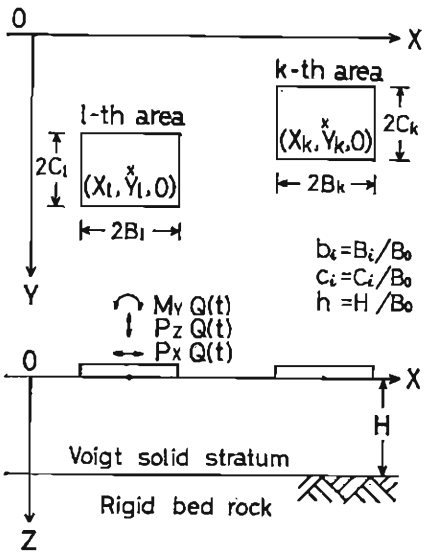

Fig. 1. Soil-foundation system considered.

k-th rectangular area with the dimensions $(2B_k \times 2C_k)$ is to be evaluated when the stress distribution in the l-th rectangular area with the dimensions $(2B_l \times 2C_l)$ is prescribed according to the following three types of force excitation: a) vertical excitation, b) horizontal excitation in the X-direction and c) rotational excitation about the principal axis of the rectangular area parallel to the Y-axis. The stress distribution in each case is given in the form of $q_j(X, Y)Q(t)$ in which subscript $j=V, H, R$ corresponds to the type of excitation. Then the boundary condition at the surface, $Z=0$, is expressed in the following form corresponding to each case:

(a) Vertical excitation

$$\tau_{ZX}=\tau_{YZ}=0$$

$$\sigma_Z=\begin{cases}0 & \text{for } |X-X_l|>B_l \text{ or } |Y-Y_l|>C_l \\ -q_{0V}\cdot Q(t) & \text{for } |X-X_l|\leq B_l \text{ and } |Y-Y_l|\leq C_l\end{cases} \tag{2.8}$$

(b) Horizontal excitation

$$\sigma_Z=\tau_{YZ}=0$$

$$\tau_{ZX}=\begin{cases}0 & \text{for } |X-X_l|>B_l \text{ or } |Y-Y_l|>C_l \\ -q_{0H}\cdot Q(t) & \text{for } |X-X_l|\leq B_l \text{ and } |Y-Y_l|\leq C_l\end{cases} \tag{2.9}$$

(c) Rotational excitation

$$\tau_{ZX}=\tau_{YZ}=0$$

$$\sigma_Z=\begin{cases}0 & \text{for } |X-X_l|>B_l \text{ or } |Y-Y_l|>C_l \\ -q_{0R}\cdot\dfrac{X}{B_l}\cdot Q(t) & \text{for } |X-X_l|\leq B_l \text{ and } |Y-Y_l|\leq C_l\end{cases} \tag{2.10}$$

The amplitude of the resultant exciting force for each case thus becomes

$$P_Z=4B_lC_lq_{0V}, \qquad P_X=4B_lC_lq_{0H}, \qquad M_Y=\frac{4}{3}B_l^2C_lq_{0R}$$

Next, the boundary condition at the interface, $Z=H$, between the stratum and the rigid bed rock is given by

$$U=V=W=0 \qquad \text{for} \qquad Z=H \tag{2.11}$$

under the assumption of welded contact of the stratum on the rigid bed rock. Equating the Fourier transform of the boundary conditions given by Eqs. (2.8) to (2.11) into the transformed displacement and stress components at the boundaries which are given by Eq. (2.2) and Eqs. (2.5) to (2.7), respectively, six equations for the arbitrary functions A_1, A_2, B_1, B_2, C_1 and C_2 are obtained. By solving these equations and substituting the solutions into Eq. (2.2), the three displacement components at any point of the Voigt stratum can be determined. The ground compliance of the k-th area corresponding to the three types of excitation to the l-th area are expressed in the following dimensionless forms:

(a) Vertical excitation

(1) Horizontal translation parallel to the X-axis

$$\begin{aligned} J_{Zl}^{Xk}&=\frac{\tilde{U}_{ave}(a_0, \boldsymbol{x}_k-\boldsymbol{x}_l)}{P_Z\tilde{Q}(a_0)}B_0\mu \\ &=\frac{a_0g_s}{\pi^2}\int_0^{\pi/2}d\theta\int_0^{\infty}d\xi\ \frac{\xi^2}{F(\xi)}\Big[\{\xi^2(2\xi^2-g_s)+2\alpha_p^2\alpha_s^2\} \\ &\quad+g_s\alpha_p\alpha_s\{\coth a_0h\alpha_p\coth a_0h\alpha_s-\operatorname{cosech}a_0h\alpha_p\operatorname{cosech}a_0h\alpha_s\}\Big] \\ &\quad\cdot\cos\theta\cdot S(a_0\xi, \theta, b_l, c_l)\cdot S(a_0\xi, \theta, b_k, c_k) \\ &\quad\cdot\sin\{a_0\xi(x_k-x_l)\cos\theta\}\cdot\cos\{a_0\xi(y_k-y_l)\sin\theta\} \end{aligned} \tag{2.12}$$

(2) Horizontal translation parallel to the Y-axis

$$\begin{aligned} J_{Zl}^{Yk}&=\frac{\tilde{V}_{ave}(a_0, \boldsymbol{x}_k-\boldsymbol{x}_l)}{P_Z\tilde{Q}(a_0)}B_0\mu \\ &=\frac{a_0g_s}{\pi^2}\int_0^{\pi/2}d\theta\int_0^{\infty}d\xi\ \frac{\xi^2}{F(\xi)}\Big[\{\xi^2(2\xi^2-g_s)+2\alpha_p^2\alpha_s^2\} \\ &\quad+g_s\alpha_p\alpha_s\{\coth a_0h\alpha_p\coth a_0h\alpha_s-\operatorname{cosech}a_0h\alpha_p\operatorname{cosech}a_0h\alpha_s\}\Big] \\ &\quad\cdot\sin\theta\cdot S(a_0\xi, \theta, b_l, c_l)\cdot S(a_0\xi, \theta, b_k, c_k) \\ &\quad\cdot\cos\{a_0\xi(x_k-x_l)\cos\theta\}\cdot\sin\{a_0\xi(y_k-y_l)\sin\theta\} \end{aligned} \tag{2.13}$$

(3) Vertical translation

$$J^{Z}_{Zl}{}^{k}=\frac{\tilde{W}_{ave}(a_0,\ \boldsymbol{x}_k-\boldsymbol{x}_l)}{P_Z\tilde{Q}(a_0)}B_0\mu$$

$$=\frac{a_0 g_s}{\pi^2}\int_0^{\pi/2}d\theta\int_0^{\infty}d\xi\ \frac{-g_s\xi\alpha_p}{F(\xi)}\left[\{\xi^2\coth a_0h\alpha_p-\alpha_p\alpha_s\coth a_0h\alpha_s\}\right.$$

$$\cdot S(a_0\xi,\ \theta,\ b_l,\ c_l)\cdot S(a_0\xi,\ \theta,\ b_k,\ c_k)$$

$$\left.\cdot\cos\{a_0\xi\,(x_k-x_l)\cos\theta\}\cdot\cos\{a_0\xi\,(y_k-y_l)\sin\theta\}\right. \tag{2.14}$$

(4) Rotation about the principal axis parallel to the Y-axis

$$J^{Z}_{Zl}{}^{X_k}=\frac{\tilde{\Phi}_{Yave}(a_0,\ \boldsymbol{x}_k-\boldsymbol{x}_l)}{P_Z\tilde{Q}(a_0)}B_0^2\mu$$

$$=\frac{a_0 g_s}{\pi^2}\int_0^{\pi/2}d\theta\int_0^{\infty}d\xi\ \frac{g_s\xi\alpha_p}{F(\xi)}\{\xi^2\coth a_0h\alpha_p-\alpha_p\alpha_s\coth a_0h\alpha_s\}$$

$$\cdot S(a_0\xi,\ \theta,\ b_l,\ c_l)\cdot N_Y(a_0\xi,\ \theta,\ b_k,\ c_k)$$

$$\cdot\sin\{a_0\xi\,(x_k-x_l)\cos\theta\}\cdot\cos\{a_0\xi\,(y_k-y_l)\sin\theta\} \tag{2.15}$$

(5) Rotation about the principal axis parallel to the X-axis

$$J^{Y}_{Zl}{}^{k}=\frac{\tilde{\Phi}_{Xave}(a_0,\ \boldsymbol{x}_k-\boldsymbol{x}_l)}{P_Z\tilde{Q}(a_0)}B_0^2\mu$$

$$=\frac{a_0 g_s}{\pi^2}\int_0^{\pi/2}d\theta\int_0^{\infty}d\xi\ \frac{g_s\xi\alpha_p}{F(\xi)}\{\xi^2\coth_0 h\alpha_p-\alpha_p\alpha_s\coth a_0h\alpha_s\}$$

$$\cdot S(a_0\xi,\ \theta,\ b_l,\ c_l)\cdot N_X(a_0\xi,\ \theta,\ b_k,\ c_k)$$

$$\cdot\cos\{a_0\xi\,(x_k-x_l)\cos\theta\}\cdot\sin\{a_0\xi\,(y_k-y_l)\sin\theta\} \tag{2.16}$$

(b) Horizontal excitation parallel to the X-axis

(1) Horizontal translation parallel to the X-axis

$$J^{X_k}_{Xl}=\frac{\tilde{U}_{ave}(a_0,\ \boldsymbol{x}_k-\boldsymbol{x}_l)}{P_X\tilde{Q}(a_0)}B_0\mu$$

$$=\frac{a_0 g_s}{\pi^2}\int_0^{\pi/2}d\theta\int_0^{\infty}d\xi\left[\frac{\xi}{\alpha_s}\tanh a_0h\alpha_s\cdot\sin^2\theta\right.$$

$$\left.-\frac{g_s\xi\alpha_s}{F(\xi)}\{\xi^2\coth a_0h\alpha_s-\alpha_p\alpha_s\coth a_0h\alpha_p\}\cdot\cos^2\theta\right]$$

$$\cdot S(a_0\xi,\ \theta,\ b_l,\ c_l)\cdot S(a_0\xi,\ \theta,\ b_k,\ c_k)$$

$$\cdot\cos\{a_0\xi\,(x_k-x_l)\cos\theta\}\cdot\cos\{a_0\xi\,(y_k-y_l)\sin\theta\} \tag{2.17}$$

(2) Horizontal translation parallel to the Y-axis

$$J^{Yk}_{Xl}=\frac{\tilde{V}_{ave}(a_0,\ \boldsymbol{x}_k-\boldsymbol{x}_l)}{P_X\bar{Q}(a_0)}B_0\mu$$

$$=\frac{a_0g_s}{\pi^2}\int_0^{\pi/2}d\theta\int_0^{\infty}d\xi\left[\frac{\xi}{\alpha_s}\tanh a_0h\alpha_s+\frac{g_s\xi\alpha_s}{F(\xi)}\{\xi^2\coth a_0h\alpha_s\right.$$

$$\left.-\alpha_p\alpha_s\coth a_0h\alpha_p\}\right]$$

$$\cdot\cos\theta\cdot\sin\theta\cdot S(a_0\xi,\ \theta,\ b_l,\ c_l)\cdot S(a_0\xi,\ \theta,\ b_k,\ c_k)$$

$$\cdot\sin\{a_0\xi(x_k-x_l)\cos\theta\}\cdot\sin\{a_0\xi(y_k-y_l)\sin\theta\} \tag{2.18}$$

(3) Vertical translation

$$J^{Zk}_{Xl}=\frac{\tilde{W}_{ave}(a_0,\ \boldsymbol{x}_k-\boldsymbol{x}_l)}{P_X\bar{Q}(a_0)}B_0\mu$$

$$=\frac{a_0g_s}{\pi^2}\int_0^{\pi/2}d\theta\int_0^{\infty}d\xi\,\frac{-\xi^2}{F(\xi)}[\{\xi^2(2\xi^2-g_s)+2\alpha_p^2\alpha_s^2\}$$

$$+g_s\alpha_p\alpha_s\{\coth a_0h\alpha_p\coth a_0h\alpha_s-\operatorname{cosech}a_0h\alpha_p\operatorname{cosech}a_0h\alpha_s\}]$$

$$\cdot\cos\theta\cdot S(a_0\xi,\ \theta,\ b_l,\ c_l)\cdot S(a_0\xi,\ \theta,\ b_k,\ c_k)$$

$$\cdot\sin\{a_0\xi(x_k-x_l)\cos\theta\}\cdot\cos\{a_0\xi(y_k-y_l)\sin\theta\} \tag{2.19}$$

(4) Rotation about the principal axis parallel to the Y-axis

$$J^{ZX_k}_{Xl}=\frac{\tilde{\Phi}_{Yave}(a_0,\ \boldsymbol{x}_k-\boldsymbol{x}_l)}{P_X\bar{Q}(a_0)}B_0^2\mu$$

$$=\frac{a_0g_s}{\pi^2}\int_0^{\pi/2}d\theta\int_0^{\infty}d\xi\,\frac{-\xi^2}{F(\xi)}[\{\xi^2(2\xi^2-g_s)+2\alpha_p^2\alpha_s^2\}$$

$$+g_s\alpha_p\alpha_s\{\coth a_0h\alpha_p\coth a_0h\alpha_s-\operatorname{cosech}a_0h\alpha_p\operatorname{cosech}a_0h\alpha_s\}]$$

$$\cdot\cos\theta\cdot S(a_0\xi,\ \theta,\ b_l,\ c_l)\cdot N_Y(a_0\xi,\ \theta,\ b_k,\ c_k)$$

$$\cdot\cos\{a_0\xi(x_k-x_l)\cos\theta\}\cdot\cos\{a_0\xi(y_k-y_l)\sin\theta\} \tag{2.20}$$

(5) Rotation about the principal axis parallel to the X-axis

$$J^{YZ_k}_{Xl}=\frac{\tilde{\Phi}_{Xave}(a_0,\ \boldsymbol{x}_k-\boldsymbol{x}_l)}{P_X\bar{Q}(a_0)}B_0^2\mu$$

$$=\frac{a_0g_s}{\pi^2}\int_0^{\pi/2}d\theta\int_0^{\infty}d\xi\,\frac{\xi^2}{F(\xi)}[\{\xi^2(2\xi^2-g_s)+2\alpha_p^2\alpha_s^2\}$$

$$+ g_s\alpha_p\alpha_s\{\coth a_0h\alpha_p\coth a_0h\alpha_s - \operatorname{cosech} a_0h\alpha_p\operatorname{cosech} a_0h\alpha_s\}]$$
$$\cdot\cos\theta\cdot S(a_0\xi,\ \theta,\ b_l,\ c_l)\cdot N_X(a_0\xi,\ \theta,\ b_k,\ c_k)$$
$$\cdot\sin\{a_0\xi(x_k-x_l)\cos\theta\}\cdot\sin\{a_0\xi(y_k-y_l)\sin\theta\} \tag{2.21}$$

(c) Rotational excitation about the principal axis parallel to the Y-axis

(1) Horizontal translation parallel to the X-axis

$$J_{Z\,X\,l}^{X\,k}=\frac{\tilde{U}_{ave}(a_0,\ \boldsymbol{x}_k-\boldsymbol{x}_l)}{M_Y\tilde{Q}(a_0)}B_0^2\mu$$
$$=\frac{a_0g_s}{\pi^2}\int_0^{\pi/2}d\theta\int_0^{\infty}d\xi\,\frac{-\xi^2}{F(\xi)}[\{\xi^2(2\xi^2-g_s)+2\alpha_p^2\alpha_s^2\}$$
$$+ g_s\alpha_p\alpha_s\{\coth a_0h\alpha_p\coth a_0h\alpha_s - \operatorname{cosech} a_0h\alpha_p\operatorname{cosech} a_0h\alpha_s\}]$$
$$\cdot\cos\theta\cdot N_Y(a_0\xi,\ \theta,\ b_l,\ c_l)\cdot S(a_0\xi,\ \theta,\ b_k,\ c_k)$$
$$\cdot\cos\{a_0\xi(x_k-x_l)\cos\theta\}\cdot\cos\{a_0\xi(y_k-y_l)\sin\theta\} \tag{2.22}$$

(2) Horizontal translation parallel to the Y-axis

$$J_{Z\,X\,l}^{Y\,k}=\frac{\tilde{V}_{ave}(a_0,\ \boldsymbol{x}_k-\boldsymbol{x}_l)}{M_Y\tilde{Q}(a_0)}B_0^2\mu$$
$$=\frac{a_0g_s}{\pi^2}\int_0^{\pi/2}d\theta\int_0^{\infty}d\xi\,\frac{\xi^2}{F(\xi)}[\{\xi^2(2\xi^2-g_s)+2\alpha_p^2\alpha_s^2\}$$
$$+ g_s\alpha_p\alpha_s\{\coth a_0h\alpha_p\coth a_0h\alpha_s - \operatorname{cosech} a_0h\alpha_p\operatorname{cosech} a_0h\alpha_s\}]$$
$$\cdot\sin\theta\cdot N_Y(a_0\xi,\ \theta,\ b_l,\ c_l)\cdot S(a_0\xi,\ \theta,\ b_k,\ c_k)$$
$$\cdot\sin\{a_0\xi(x_k-x_l)\cos\theta\}\cdot\sin\{a_0\xi(y_k-y_l)\sin\theta\} \tag{2.23}$$

(3) Vertical translation

$$J_{Z\,X\,l}^{Z\,k}=\frac{\tilde{W}_{ave}(a_0,\ \boldsymbol{x}_k-\boldsymbol{x}_l)}{M_Y\tilde{Q}(a_0)}B_0^2\mu$$
$$=\frac{a_0g_s}{\pi^2}\int_0^{\pi/2}d\theta\int_0^{\infty}d\xi\,\frac{-g_s\xi\alpha_p}{F(\xi)}\{\xi^2\coth a_0h\alpha_p-\alpha_p\alpha_s\coth a_0h\alpha_s\}$$
$$\cdot N_Y(a_0\xi,\ \theta,\ b_l,\ c_l)\cdot S(a_0\xi,\ \theta,\ b_k,\ c_k)$$
$$\cdot\sin\{a_0\xi(x_k-x_l)\cos\theta\}\cdot\cos\{a_0\xi(y_k-y_l)\sin\theta\} \tag{2.24}$$

(4) Rotation about the principal axis parallel to the Y-axis

$$J^{ZXk}_{ZXl}=\frac{\tilde{\Phi}_{Yave}(a_0, \boldsymbol{x}_k-\boldsymbol{x}_l)}{M_Y\tilde{Q}(a_0)}B_0^3\mu$$

$$=\frac{a_0 g_s}{\pi^2}\int_0^{\pi/2}d\theta\int_0^{\infty}d\xi\,\frac{-g_s\xi\alpha_p}{F(\xi)}\{\xi^2\coth a_0h\alpha_p-\alpha_p\alpha_s\coth a_0h\alpha_s\}$$

$$\cdot N_Y(a_0\xi, \theta, b_l, c_l)\cdot N_Y(a_0\xi, \theta, b_k, c_k)$$

$$\cdot\cos\{a_0\xi(x_k-x_l)\cos\theta\}\cdot\cos\{a_0\xi(y_k-y_l)\sin\theta\} \tag{2.25}$$

(5) Rotation about the principal axis parallel to the X-axis

$$J^{YZk}_{ZXl}=\frac{\tilde{\Phi}_{Xave}(a_0, \boldsymbol{x}_k-\boldsymbol{x}_l)}{M_Y\tilde{Q}(a_0)}B_0^3\mu$$

$$=\frac{a_0 g_s}{\pi^2}\int_0^{\pi/2}d\theta\int_0^{\infty}d\xi\,\frac{g_s\xi\alpha_p}{F(\xi)}\{\xi^2\coth a_0h\alpha_p-\alpha_p\alpha_s\coth a_0h\alpha_s\}$$

$$\cdot N_Y(a_0\xi, \theta, b_l, c_l)\cdot N_X(a_0\xi, \theta, b_k, c_k)$$

$$\cdot\sin\{a_0\xi(x_k-x_l)\cos\theta\}\cdot\sin\{a_0\xi(y_k-y_l)\sin\theta\} \tag{2.26}$$

In the above equations, the dimensionless frequency a_0, the dimensionless coordinates $\boldsymbol{x}$ and the dimensionless half lengths b_i and c_i of the i-th rectangular area are used, which are respectively defined as

$$a_0=\frac{\omega B_0}{V_s},\quad \boldsymbol{x}=\{x, y, z\}=\left\{\frac{X}{B_0}, \frac{Y}{B_0}, \frac{Z}{B_0}\right\},\quad b_i=\frac{B_i}{B_0},\quad c_i=\frac{C_i}{B_0} \tag{2.27}$$

where B_0 denotes the reference value of length.

And, the dimensionless functions appearing in Eqs. (2.12) to (2.26) are defined as follows:

$$F(\xi)=\xi^2\{(2\xi^2-g_s)^2+4\alpha_p^2\alpha_s^2\}$$

$$-\alpha_p\alpha_s\{(2\xi^2-g_s)^2+4\xi^4\}\coth a_0h\alpha_p\cdot\coth a_0h\alpha_s$$

$$+4\alpha_p\alpha_s\xi^2(2\xi^2-g_s)\operatorname{cosech}a_0h\alpha_p\cdot\operatorname{cosech}a_0h\alpha_s \tag{2.28}$$

$$S(a_0\xi, \theta, b_i, c_i)=\frac{\sin(b_ia_0\xi\cos\theta)}{b_ia_0\xi\cos\theta}\cdot\frac{\sin(c_ia_0\xi\sin\theta)}{c_ia_0\xi\sin\theta}$$

$$N_X(a_0\xi, \theta, b_i, c_i)=\frac{3}{c_i}\cdot\frac{\sin(b_ia_0\xi\cos\theta)}{b_ia_0\xi\cos\theta}\left\{\frac{\sin(c_ia_0\xi\sin\theta)}{(c_ia_0\xi\sin\theta)^2}-\frac{\cos(c_ia_0\xi\sin\theta)}{c_ia_0\xi\sin\theta}\right\}$$

$$N_Y(a_0\xi, \theta, b_i, c_i)=\frac{3}{b_i}\cdot\left\{\frac{\sin(b_ia_0\xi\cos\theta)}{(b_ia_0\xi\cos\theta)^2}-\frac{\cos(b_ia_0\xi\cos\theta)}{b_ia_0\xi\cos\theta}\right\}\frac{\sin(c_ia_0\xi\sin\theta)}{c_ia_0\xi\sin\theta}$$

$$i=l, k \tag{2.29}$$

and

$$\alpha_p=\sqrt{\xi^2-n^2 g_p}, \qquad \alpha_s=\sqrt{\xi^2-g_s}$$

$$g_p=\frac{1}{1+j\omega d_p}=\frac{1}{1+ja_0\eta_p}, \qquad g_s=\frac{1}{1+j\omega d_s}=\frac{1}{1+ja_0\eta_s}$$

$$\eta_p=\frac{V_s}{B_0}\,\frac{\lambda'+2\mu'}{\lambda+2\mu}=n^2\eta_s\left(2+\frac{\lambda'}{\mu'}\right), \qquad \eta_s=\frac{V_s}{B_0}\,\frac{\mu'}{\mu}$$

$$n^2=\frac{\mu}{\lambda+2\mu}=\left(\frac{V_s}{V_p}\right)^2=\frac{1-2\nu}{2(1-\nu)}, \qquad h=\frac{H}{B_0} \tag{2.30}$$

In Eqs. (2.12) to (2.26), the notation $J_{\mu l}^{\lambda k}$ shows the λ-component of compliance associated with the k-th area due to the μ type excitation to the l-th area. The symbol $\sim$ denotes the Fourier transform with respect to the dimensionless time $\tau=tV_s/B_0$, and the subscript *ave* means the following average weighted by the stress distribution:

$$\tilde{U}_{ave}(a_0, \boldsymbol{x}_k-\boldsymbol{x}_l)=\iint_{D_k}\tau_{ZX}(\boldsymbol{x})\tilde{U}(a_0, \boldsymbol{x}-\boldsymbol{x}_l)dxdy\Big/\iint_{D_k}\tau_{ZX}(\boldsymbol{x})dxdy$$

$$\tilde{V}_{ave}(a_0, \boldsymbol{x}_k-\boldsymbol{x}_l)=\iint_{D_k}\tau_{YZ}(\boldsymbol{x})\tilde{V}(a_0, \boldsymbol{x}-\boldsymbol{x}_l)dxdy\Big/\iint_{D_k}\tau_{YZ}(\boldsymbol{x})dxdy$$

$$\tilde{W}_{ave}(a_0, \boldsymbol{x}_k-\boldsymbol{x}_l)=\iint_{D_k}\sigma_Z(\boldsymbol{x})\,\tilde{W}(a_0, \boldsymbol{x}-\boldsymbol{x}_l)dxdy\Big/\iint_{D_k}\sigma_Z(\boldsymbol{x})dxdy$$

$$\tilde{\Phi}_{Yave}(a_0, \boldsymbol{x}_k-\boldsymbol{x}_l)=\iint_{D_k}\sigma_Z(\boldsymbol{x})\,\tilde{W}(a_0, \boldsymbol{x}-\boldsymbol{x}_l)\,dxdy\Big/\iint_{D_k}(x-x_l)\sigma_Z(\boldsymbol{x})dxdy$$

$$\tilde{\Phi}_{Xave}(a_0, \boldsymbol{x}_k-\boldsymbol{x}_l)=\iint_{D_k}\sigma_Z(\boldsymbol{x})\,\tilde{W}(a_0, \boldsymbol{x}-\boldsymbol{x}_l)\,dxdy\Big/\iint_{D_k}(y-y_l)\sigma_Z(\boldsymbol{x})dxdy \tag{2.31}$$

The function $F(\xi)$ in Eq. (2.28) is the dimensionless frequency equation of the Rayleigh waves of the visco-elastic stratum on the rigid bed rock. And, the functions S, N_X and N_Y in Eq. (2.29) represent the contribution of the uniform stress distribution in the cases of vertical and horizontal excitations and those of the triangular stress distributions in the cases of the rotations about the principal axis parallel to the X- and Y-axis, respectively. It is noted that the function $\tanh a_0 h\alpha_s$ in Eqs. (2.17) and (2.18) for the cases of horizontal translations due to horizontal excitation is the inverse of the dimensionless frequency equation of the Love waves of the visco-elastic stratum on the rigid bed rock.

2.2 Numerical Examples of the Ground Compliance

The dimensionless ground compliances of the rectangular foundation on a visco-elastic stratum on the rigid bed rock defined by Eqs. (2.12) to (2.26) are evaluated

Table. Specifications of Figures 2 and 3.

Fig. number	relative coordinates $x_k - x_l$	component of compliance λ	type of excitation μ
2(a)	{0, 0, 0}	vertical (Z)	vertical (Z)
2(b)	{0, 0, 0}	horizontal (X)	horizontal (X)
2(c)	{0, 0, 0}	rotational (ZX)	rotational (ZX)
2(d)	{0, 0, 0}	rotational (ZX)	horizontal (X)
3(a)	{4, 0, 0}	vertical (Z)	vertical (Z)
3(b)	{4, 0, 0}	horizontal (X)	horizontal (X)
3(c)	{4, 0, 0}	rotational (ZX)	rotational (ZX)
3(d)	{4, 0, 0}	rotational (ZX)	horizontal (X)
3(e)	{4, 0, 0}	rotational (ZX)	vertical (Z)
3(f)	{4, 0, 0}	horizontal (X)	vertical (Z)

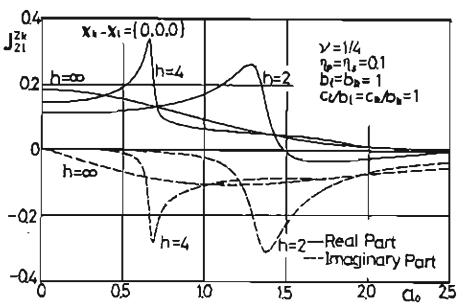

(a) Vertical (Z) component to vertical (Z) excitation.

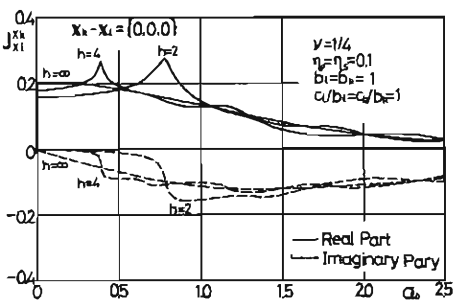

(b) Horizontal (X) component to horizontal (X) excitation.

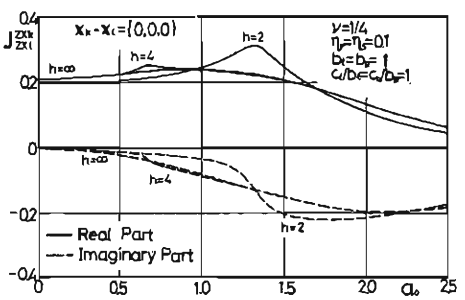

(c) Rotational (ZX) component to rotational (ZX) excitation.

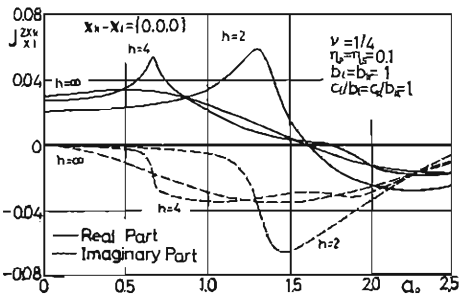

(d) Rotational (ZX) component to horizontal (X) excitation.

Fig. 2. Ground compliances of square foundation area, $x_k - x_l = \{0, 0, 0\}$

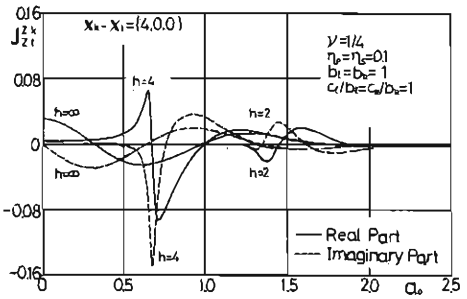

(a) Vertical (Z) component to vertical (Z) excitation.

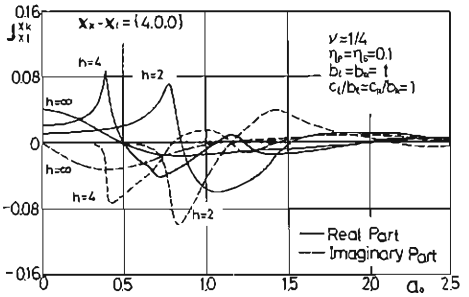

(b) Horizontal (X) component to horizontal (X) excitation.

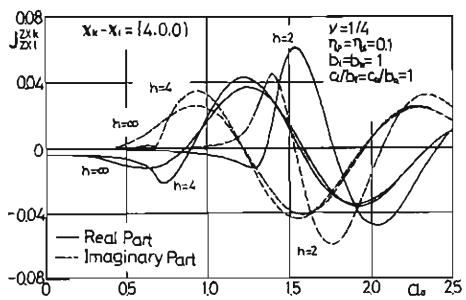

(c) Rotational (ZX) component to rotational (ZX) excitation.

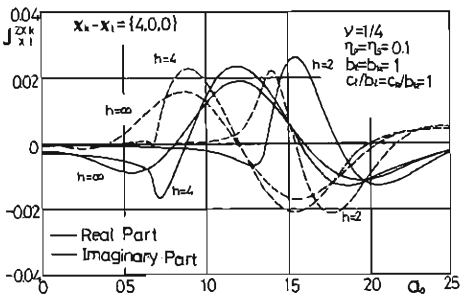

(d) Rotational (ZX) component to horizontal (X) excitation.

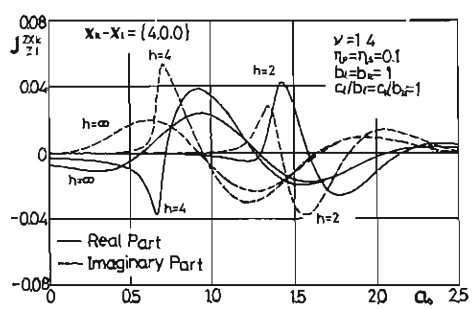

(e) Rotational (ZX) component to vertical (Z) excitation

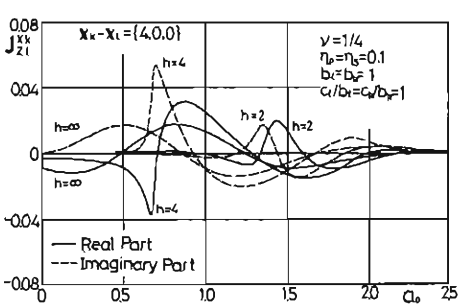

(f) Horizontal (X) component to vertical (Z) excitation.

Fig. 3. Ground compliances of square foundation area, $x_k - x_l = \{4, 0, 0\}$

numerically in the cases where the dimensionless thickness of the stratum $h=2$, 4 and ∞. It is assumed that the Poisson's ratio of the stratum $\nu=1/4$, the dimensionless viscosity coefficients $\eta_s=\eta_p=0.1$, and both the k-th and l-th foundation have the

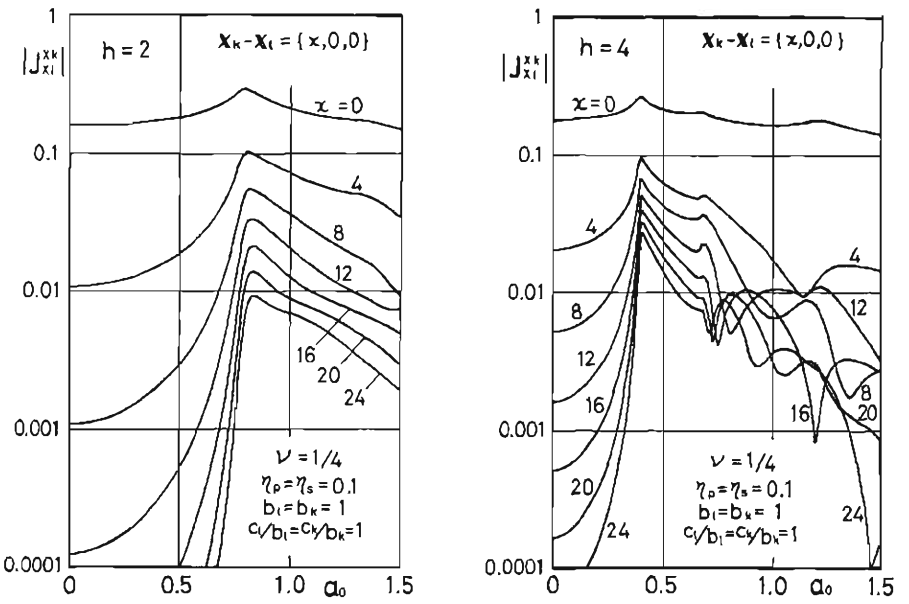

(a) $h=2$. (b) $h=4$.

Fig. 4. Absolute values of the horizontal component of ground compliances to horizontal excitation.

identical square areas being along the X-axis at the surface of the stratum. The halflength of the side of the square areas is taken as the reference value of length, namely, $B_l=B_k=B_0$ or $b_l=b_k=1$. The numerical results of the ground compliances are shown in Figs. 2 and 3, where the solid and broken curves correspond respectively to the real and imaginary parts of the dimensionless ground compliances. The dimensionless relative coordinates, $\boldsymbol{x}_k-\boldsymbol{x}_l$, of the center of the k-th area to that of the l-th area, the component of compliance λ and the type of excitation μ in these figures are shown in Table.

From Figs. 2 and 3, it is found that in the case of stratum, the radiation damping is very small in the frequency range lower than the lowest resonance frequency of the stratum and that the effect of the thickness of stratum on the ground compliance is stronger in order of vertical, horizontal and rotational excitations. And also it is shown that the resonance frequencies of the horizontal component due to the horizontal excitation are lower than those of other cases because the Love type waves may be predominant in the former case and the Rayleigh type waves in the latter cases.

As shown in Figs. 3(e) and (f), in the case where $\boldsymbol{x}_k-\boldsymbol{x}_l=\{4, 0, 0\}$, the rotational component $J^{\theta x}_{z}$ about the principal axis parallel to the Y-axis and the horixontal component J^{x}_{z} in the X-direction due to the vertical excitation are generated mainly by the Rayleigh type waves. In Figs. 3(a) to (f), it is shown that the ground compliances on the surface apart from the exciting area vary rapidly with the increase of the frequency parameter, and also that the rotational component becomes large when the frequency parameter exceeds the lowest resonance frequency of the Ray-

leigh type. In Figs. 4(a) and (b) the absolute values of the X-direction horizontal component of ground compliance $|J_K^x|$ to the horizontal excitation in the X-direction are shown for the cases where $h=2$ and 4, respectively, varying the dimensionless distance $x=|x_k-x_l|$ from 0 to 24. From these figures, it is found that in the frequency range lower than the fundamental natural frequency of the stratum, the absolute values of the ground compliance increase sharply in the vicinity of the fundamental frequency as the distance becomes large, whereas in the higher frequency range the absolute values seem to decay almost at the same rate with increase of frequency parameter regardless of the value of distance. It is noted, however, that the variation of the absolute values of ground compliance are moderate in the wide frequency range for the case where $X=0$, and also that in the case of thick stratum their variation in the higher frequency range are very complicated due to the interference of the various waves of different types and of different passes when the distance becomes large.

3. Transfer Functions of Soil-Structure Cross-Interaction Systems

The dynamical characteristics of a soil-structure cross-interaction system consisting of L-number of structures which are along the X-axis on the surface of a viscoelastic stratum over the rigid bed rock are now considered. Two kinds of excitations to the soil-structure system are supposed here, one of which is the displacement excitation at the free surface of the stratum or at the soil-rock interface, and the other is the force excitation at one of the basement masses of the structural system. For the sake of simplicity, only the X-direction horizontal components of the excitations and responses are considered. Therefore, it is assumed that the vertical and rotational components of the response of the structural system are restrained by an appropriate foundation structure. The model of the structural system considered here is the multi-mass system or the shear type multi-spring-mass system as shown in Figs. 5, 6, 13 and 17. All the dynamical characteristics of the soil-structure system are discussed in the form of dimensionless transfer functions. In defining dimensionless quantities, B_0, $B_0^3\rho$ and B_0/V_s are chosen as the basic reference values concerning length, mass and time, respectively.

In order to obtain the overall transfer function of displacement response of the soil-structure system, the following four basic dimensionless transfer functions are introduced; first, the displacement transfer function $G_B^S(ja_0)$ of the free surface to the displacement excitation at the soil-rock interface, secondly, the displacement transfer function ${}_iG_0^j(ja_0)$ of the j-th level of the i-th structure to the displacement excitation at the basement mass, thirdly, the displacement transfer function ${}_iG_S^0(ja_0)$ of the basement mass to the displacement excitation at the free surface of the stratum, and finally the displacement transfer function ${}_iG_l^0(ja_0)$ of the basement mass of the i-th structure to the force excitation applied to the basement mass of the l-th structure. Making use of the above-mentioned transfer functions, the overall dimensionless transfer functions of the soil-structure system are expressed as follows:

1) The displacement transfer function of the j-th level of the i-th structure to the displacement excitation at the free surface of the stratum, ${}_iG_S^j(ja_0)$

$$ {}_iG_S^j(ja_0)={}_iG_0^j(ja_0)\cdot{}_iG_S^0(ja_0) \tag{3.1}$$

2) The displacement transfer function of the j-th level of the i-th structure to the displacement excitation at the soil-rock interface, ${}_iG_B^j(ja_0)$

$$ {}_iG_B^j(ja_0) = {}_iG_S^j(ja_0) \cdot G_B^S(ja_0) \tag{3.2} $$

3) The displacement transfer function of the j-th level of the i-th structure to the force excitation applied to the basement mass of the l-th structure, ${}_iG_l^j(ja_0)$

$$ {}_iG_l^j(ja_0) = {}_iG_0^j(ja_0) \cdot {}_iG_l^0(ja_0) \tag{3.3} $$

In the above equations, $j=\sqrt{-1}$, a_0 denotes the dimensionless frequency, the left subscript means the number of structure, the right superscript and subscript represent the position of response and that of excitation, respectively. The basic dimensionless transfer functions appearing in Eqs. (3.1) to (3.3) are derived below.

3.1 Displacement transfer function of the stratum, $G_B^S(ja_0)$

The dimensionless displacement transfer function of the free surface of the Voigt type visco-elastic stratum to the uniform displacement excitation at the soil-rock interface is given by the following one-dimensional form[19]:

$$ G_B^S(ja_0) = \frac{2\exp\{-ja_0h\sqrt{1/(1+ja_0\eta_s)}\}}{1+\exp\{-2ja_0h\sqrt{1/(1+ja_0\eta_s)}\}} \tag{3.4} $$

3.2 The displacement transfer function of the structural system, ${}_iG_0^j(ja_0)$

The model of the individual structure of the multi-structural system is supposed to be a shear type lumped spring-mass system as shown in Fig. 5. The degrees of freedom of the i-th structure are assumed to be N_i+1 including its basement mass. The Fourier transformed equations of motion in the fixed coordinates are expressed as

$$ ({}_i[\hat{k}] - a_0^2\,{}_i[m])\,{}_i\{\tilde{u}\} = {}_i\{\chi\}\,\tilde{u}_i^0, \qquad i=1,2,\cdots,L \tag{3.5} $$

in which

$$ {}_i\{\tilde{u}\} = \begin{Bmatrix} \tilde{u}_i^{N_i} \\ \vdots \\ \tilde{u}_i^1 \end{Bmatrix} \qquad {}_i[m] = \begin{bmatrix} m_i^1 & & 0 \\ & m_i^2 & \\ 0 & & m_i^{N_i} \end{bmatrix} $$

$$ {}_i\{\chi\} = \begin{Bmatrix} \hat{k}_i^1 \\ 0 \\ \vdots \\ 0 \end{Bmatrix} \qquad {}_i[\hat{k}] = \begin{bmatrix} \hat{k}_i^1+\hat{k}_i^2 & -\hat{k}_i^2 & \cdots\cdots & 0 \\ \cdots\cdots & & & \\ & -\hat{k}_i^j & \hat{k}_i^j+\hat{k}_i^{j+1} & -\hat{k}_i^{j+1} \\ & & \cdots\cdots & \\ 0 & \cdots\cdots & -\hat{k}_i^{N_i} & \hat{k}_i^{N_i} \end{bmatrix} $$

$$ \hat{k}_i^j = k_i^j + ja_0c_i^j \tag{3.6} $$

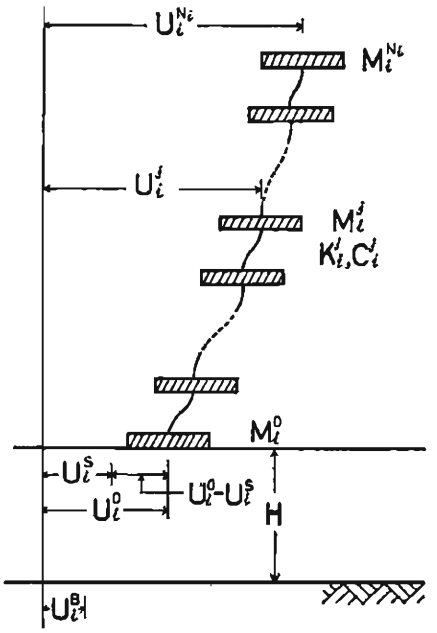

Fig. 5. Soil-structure system considered.

and

$$u_i^j = \frac{U_i^j}{B_0}, \qquad m_i^j = \frac{M_i^j}{B_0^3 \rho}, \qquad c_i^j = \frac{C_i^j}{B_0^2 \sqrt{\rho \mu}}, \qquad k_i^j = \frac{K_i^j}{B_0 \mu} \tag{3.7}$$

In the above equations, U_i^j, M_i^j, C_i^j and K_i^j are the displacement, mass, viscous damping coefficient and shear stiffness of the j-th level of the i-th structure. Solving Eq. (3.5), the dimensionless displacement transfer functions ${}_iG_0^j(ja_0)$ are obtained as follows:

$${}_i\{G\} \equiv \{{}_iG_0^j\} = \frac{{}_i\{\tilde{u}\}}{\tilde{u}_i^0} = ({}_i[\hat{k}] - a_0^2 \, {}_i[m])^{-1} \, {}_i\{x\} \tag{3.8}$$

3.3 The displacement transfer functions of the soil-structure system, ${}_iG_s^0(ja_0)$ and ${}_iG_i^0(ja_0)$

The basic responses of the soil-structural system are the displacement vector and force vector of the L-number of connecting points between the multi-structural system and stratum. The Fourier transform of the dimensionless force r_i^0 transmitted to the i-th connecting point from the i-th structure subjected to the dimensionless force f_i^0 at the basement mass is given by

$$\tilde{r}_i^0 = \{a_0^2 m_i^0 + \hat{k}_i^1 ({}_iG_0^1 - 1)\} \tilde{u}_i^0 + \tilde{f}_i^0 \tag{3.9}$$

where

$$u_i^0=\frac{U_i^0}{B_0},\qquad r_i^0=\frac{R_i^0}{B_0^2\mu},\qquad m_i^0=\frac{M_i^0}{B_0^3\rho},\qquad f_i^0=\frac{F_i^0}{B_0^2\mu} \tag{3.10}$$

In the above equations, U_i^0, R_i^0 are the displacement and force of the i-th connecting point and M_i^0, F_i^0 denote the basement mass and the force acting on it.

On the other hand, the dimensionless force vector $\{r\}^0$ can be expressed in terms of the dimensionless displacement $\{u\}^0$, the dimensionless uniform displacement excitation u^s at the free surface of the stratum and the ground compliance matrix $[J]$ as follows:

$$\{\tilde{r}\}^0=[J]^{-1}(\{\tilde{u}\}^0-\{1\}\tilde{u}^S) \tag{3.11}$$

where

$$[J]\equiv[J_l^k]=[J_X^k] \tag{3.12}$$

Representing Eq. (3.9) in the vector-matrix from,

$$\{\tilde{r}\}^0=[S]\{\tilde{u}\}^0+\{\tilde{f}\}^0 \tag{3.13}$$

where

$$[S]=\begin{bmatrix} a_0^2m_1^0+\hat{k}_1^1({}_1G_0^1-1) & & 0 \\ & \cdots\cdots & \\ & a_0^2m_i^0+\hat{k}_i^1({}_iG_0^1-1) & \\ & \cdots\cdots & \\ 0 & & a_0^2m_L^0+\hat{k}_L^1({}_LG_0^1-1) \end{bmatrix} \tag{3.14}$$

and equating Eq. (3.11) to Eq. (3.13), the transformed input-output relation in the dimensionless frequency domain is obtained as follows:

$$([I]-[J][S])\{\tilde{u}\}^0=\{1\}\tilde{u}^S+[J]\{\tilde{f}\}^0 \tag{3.15}$$

in which $[I]$ is the identity matrix and $\{1\}=\{1, 1, \ldots, 1\}^T$. The element J_l^k in the matrix $[J]$ in Eq. (3.12) means the dimensionless ground compliance of the k-th area due to the force excitation on the l-th area. The matrix $[S]$ defined by Eq. (3.14) is the dimensionless force transfer matrix of the connecting points to the displacement excitation at the points. In the case of the soil-structure system consisting of the independent structures, the matrix $[S]$ is a diagonal matrix as shown in Eq. (3.14). The solution of Eq. (3.15) is given by

$$\{u\}^0=([I]-[J][S])^{-1}(\{1\}\tilde{u}^S+[J]\{\tilde{f}\}^0) \tag{3.16}$$

By substituting $\{\tilde{f}\}^0=\{0\}$ into Eq. (3.16), the dimensionless displacement transfer vector $\{G\}_S^0$ of the connecting points to the uniform displacement excitation u^s at the free surface of the stratum is obtained as follows:

$$\{G\}_S^0\equiv\{{}_iG_S^0(ja_0)\}=\frac{\{\tilde{u}\}^0}{\tilde{u}^S}=([I]-[J][S])^{-1}\{1\} \tag{3.17}$$

On the other hand, by putting $\tilde{u}^s=0$ and $\{\tilde{f}\}^0=\{0\cdots\tilde{f}_l^0\cdots 0\}$ in Eq. (3.16), the dimensionless displacement transfer vector $\{G\}_l^0$ of the connecting points to the force excitation f_l^0 at the basement mass of the l-th structure is written as follows:

$$\{G\}_l^0 \equiv \{{}_iG_l^0(ja_0)\} = \frac{\{\tilde{u}\}^0}{\tilde{f}_l^0} = ([I]-[J][S])^{-1}\{J\}_l \tag{3.18}$$

in which $\{J\}_l$ is the l-th column of the dimensionless ground compliance matrix $[J]$.

In the case where the model of the structural system is idealized a multi-mass system, the matrix $[S]$ in Eq. (3.14) is simply expressed as follows:

$$[S]=\begin{bmatrix} a_0^2 m_1 & & 0 \\ & \ddots & \\ & a_0^2 m_i & \\ & & \ddots \\ 0 & & a_0^2 m_L \end{bmatrix}, \qquad m_i=\sum_{j=0}^{N_i} m_i^j \tag{3.19}$$

3.3 Numerical examples and discussions

The model of the soil-structure cross-interaction system used in the numerical analysis consist of the visco-elastic stratum over the rigid bed rock and the multi-mass or multi-spring-mass system which are in uniform space along the x-axis on the surface of the stratum. The visco-elastic stratum is supposed to be the Voigt solid with the Poisson's ratio $\nu=1/4$, the dimensionless viscosity coefficients $\eta_p=\eta_s=0.1$ and the dimensionless thickness $h=2$, 4, 10 or ∞. The structural system is idealized as the identical two- or seven-mass system or the two-spring-mass system each of which has a square foundation with sides parallel to the x- or y-axis. For the sake of comparison, the single mass and the single spring-mass system are considered.

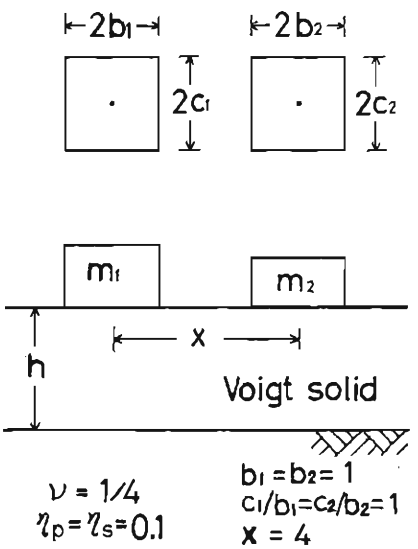

Fig. 6. Two-mass system.

The dynamical characteristics of the soil-structure cross-interaction system are studied in the form of dimensionless transfer functions associated with the displacement responses of the soil-structure system subjected to the two types of excitation one of which is the force excitation acting on one of the mass or basement masses of the system and the other is the uniform displacement excitation at the free surface of the stratum. In the case of the force excitation, the structure subjected to the force is called the active structure whereas the structures other than active one are called the passive structures[15]. Without loss of essential features of the problem, only the horizontal components in the x-direction are considered for both the response and excitation, because the horizontal components of the earthquake response of structures have been regarded as one of the most important measures for the aseismic design and the structures on the soft stratum used to be supported by the piles having the large vertical stiffness as compared with horizontal one. And also, only the amplitude characteristics of the transfer functions are shown in graphical forms because of their primary significance in estimating the dynamical characteristics.

At first, as shown in Fig. 6, the identical two-mass system subjected to the force excitation is considered as the simplest cross-interaction system, and the transfer functions of the displacements of both the active and passive masses are evaluated in the case of dimensionless distance $x=4$. Figs. 7(a) to (d) and Figs. 8(a) to (d) show the displacement amplitude characteristics $|{}_1G_1^1|$ of the active mass and those $|{}_2G_1^1|$ of the passive mass in the cases where (a) $h=2$, (b) $h=4$, (c) $h=10$ and (d) $h=\infty$, respectively. In Figs. 7 and 8, the displacement amplitude characteristics of the single mass system and those corresponding to the foundation area of the passive mass at the free surface are respectively shown by the dotted curves. From these figures, it is indicated that the displacement transfer function of a structure to the force excitation is remarkably influenced by the existence of the adjacent structure particularly in the cases of relatively shallow strata. It is also found that the cross-interaction effects are considerably different in the frequency ranges lower and higher than the fundamental natural frequency of the stratum. The fundamental natural frequency ${}_0a_{01}$ of the stratum, which is caused by the multiple reflection of S-waves, is given by $\pi/2h$, and the values of ${}_0a_{01}$ are 0.785, 0.393, 0.157, and 0, respectively, for dimensionless thickness $h=2$, 4, 10 and ∞. As found from Figs. 2 to 4, the radiation damping is small in the lower frequency range than the fundamental natural frequency of the stratum and large in the higher frequency range except the neighbourhood of the natural frequencies of the stratum. It has been known that the increase of dimensionless mass, which is called mass ratio hereafter, makes the critical damping ratio as well as the fundamental frequency of the soil-structure system decrease. Hence, as shown in Fig. 7, if the mass ratio is so large that the fundamental natural frequency of the soil-structure system becomes comparatively smaller than that of the stratum, the displacement amplitude characteristics are shape and their peak values are considerably large. On the contrary, if the mass ratio is sufficiently small to make the fundamental natural frequency of the soil-structure system a little smaller than that of the stratum, the displacement amplitude characteristics become rather flat and their peak values, appearing in the vicinities of the natural frequencies of the stratum and those mainly due to the interaction between structures and their sub-soil, are relatively small due to high damping characteristics in the higher frequency range. From Fig. 7 it is found that the effects of the cross-interaction on the displacement

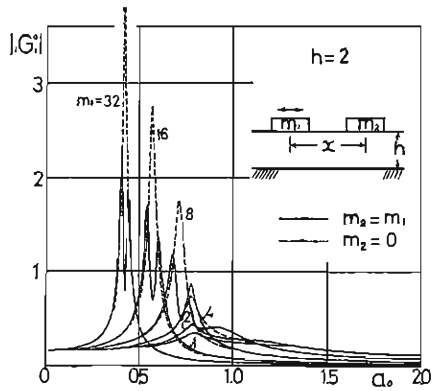

(a) $h=2$.

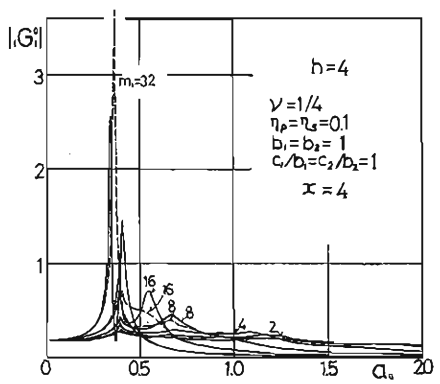

(b) $h=4$.

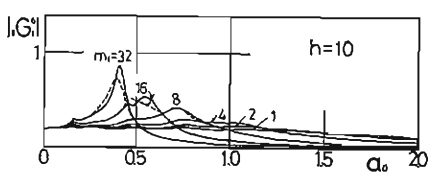

(c) $h=10$.

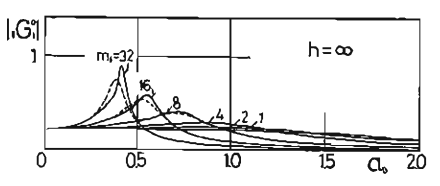

(d) $h=\infty$.

Fig. 7. Displacement amplitude characteristics of the active mass of two mass system to force excitation.

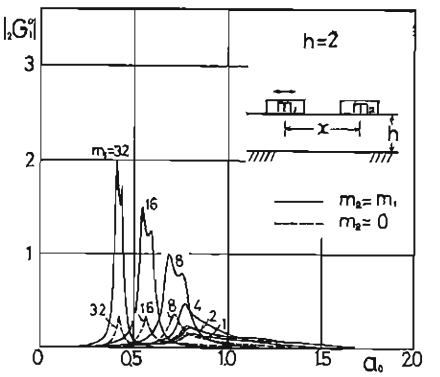

(a) $h=2$.

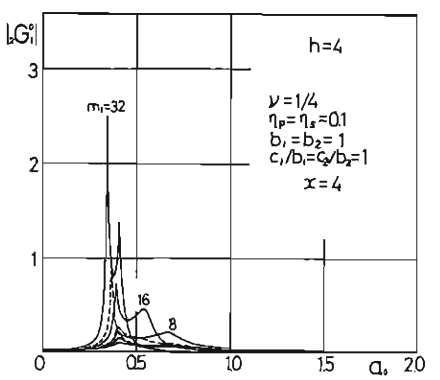

(b) $h=4$.

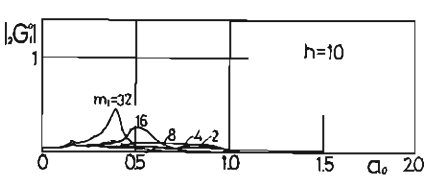

(c) $h=10$.

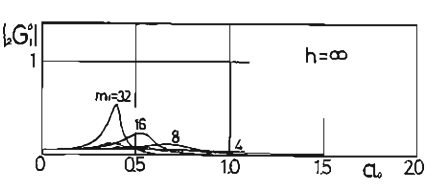

(d) $h=\infty$.

Fig. 8. Displacement amplitude characteristics of the passive mass of two-mass system to force excitation.

amplitude characteristics of the active mass are remarkable in the lower frequency range, particularly in the cases where $h=2$ and 4. Consequently, the general features of the displacement amplitude characteristics of the two-mass system become quite different from those of the single mass system. In the case of the cross-interaction system composed of dual identical masses, two natural frequencies appear in the vicinity of the natural frequency of the single mass system. The vibrational mode having the lower frequency seems to be of the in-phase type and the other mode having the higher frequency may be of the out-of-phase type, although this classification of modes can not exactly be applicable to the soil-structure system in which the so-called modal coupling does occur. As shown in Figs. 7(a) and (b) in the frequency range lower than the fundamental natural frequency of the stratum, the peak values of the active mass of the two-mass system are considerably smaller than the peak value of the single mass system becuase of the interference between the above-mentioned two vibrational modes. As indicated in Figs. 7(a) to (d), however, in the frequency range higher than the fundamental natural frequency of the stratum, the peak values of the two-mass system are somewhat larger than those of the single mass system since the lower vibrational modes near the surface are rather similar and the heavy modal coupling may occur between these modes. It is also found that as the frequency increases the general features of the transfer functions of the two-mass system become almost similar to those of the single mass system becuase of the contribution of the waves having comparatively short wave length. Hence, in the higher frequency range the effects of the thickness of stratum and of the distance between structures may be trivial especially for the active mass. With regard to the passive mass of the identical two-mass system, as shown in Fig. 8(a) to (d), it is noted that when the mass ratio is large, the values of the displacement amplitude characteristics of the passive mass of the two-mass system are of the same order to those of the active mass in the vicinities of the resonance frequencies almost regardless of the thickness of the stratum, since the cross-interaction is remarkable due to the coincidence of the resonance frequencies of individual structure-subsoil system.

Figs. 9 and 10 show the effects of the distance between two identical masses on the displacement amplitude characteristics $|{}_1G_1^1|$ of the active mass and those $|{}_2G_1^1|$ of the passive mass, respectively, in the case where $h=2$. Figs. 11 and 12 are the same figures in the case where $h=4$. From Figs. 9 and 11, it is found that when the mass ratio is large, the effects of distance on the displacement amplitude characteristics of the active mass is remarkable in the frequency range including the lower natural frequencies of the soil-structure system, and also indicated that the effects of distance on the amplitude characteristics of the active mass decrease as the mass ratio becomes small and the thickness of stratum becames large. From Figs. 10 and 12, however, it is shown that the effects of distance on the displacement amplitude characteristics of the passive mass are significant even in the case where the mass ratio is sufficiently small and the thickness of stratum is comparatively large. Also, Figs. 9 to 12 show that when the mass ratio is small and the lowest natural frequency due to the interaction between structure and its surrounding sub-soil exceeds the fundamental natural frequency of the stratum the effects of distance appear in broad frequency range, because of the increase of damping and of the strong modal coupling in the higher frequency range. It is also indicated that when the natural frequency of the structure-subsoil system is in the higher frequency range, the resonance frequency in the neigh-

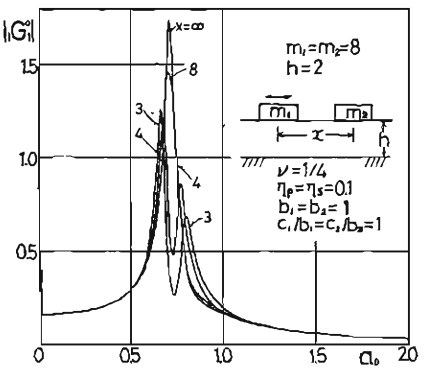

(a) $m_1=m_2=8$.

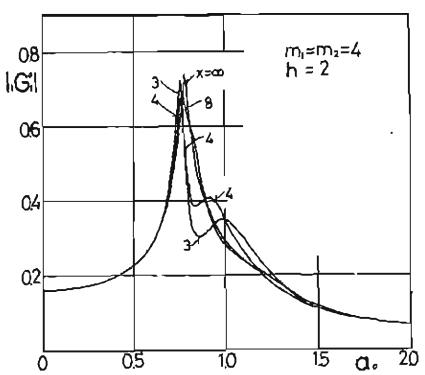

(b) $m_1=m_2=4$.

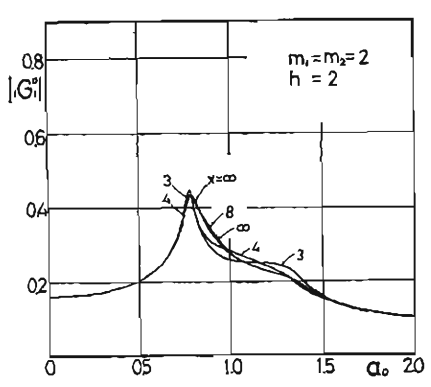

(c) $m_1=m_2=2$.

Fig. 9. Displacement amplitude characteristics of the active mass of two-mass system to force excitation, $h=2$.

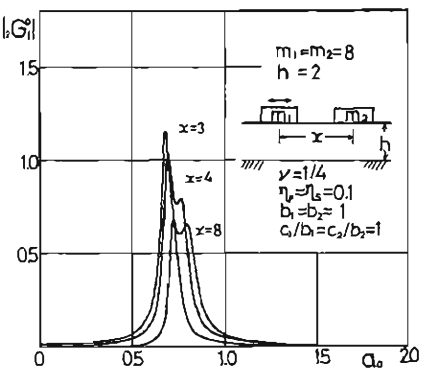

(a) $m_1=m_2=8$.

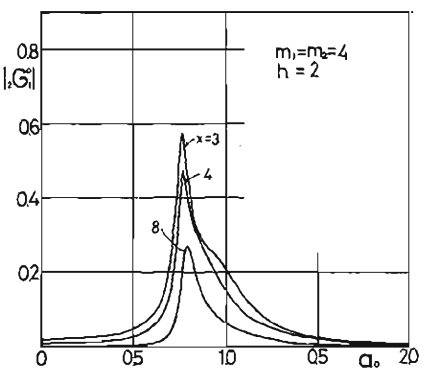

(b) $m_1=m_2=4$.

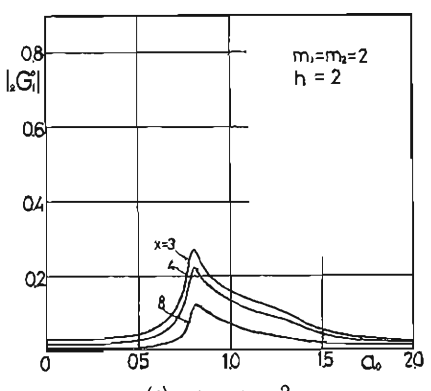

(c) $m_1=m_2=2$.

Fig. 10. Displacement amplitude characteristics of the passive mass of two-mass system to force excitation, $h=2$.

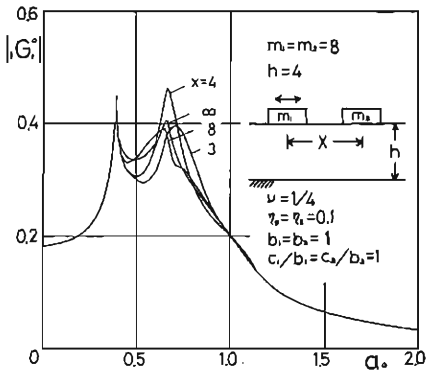

(a) $m_1=m_2=8$.

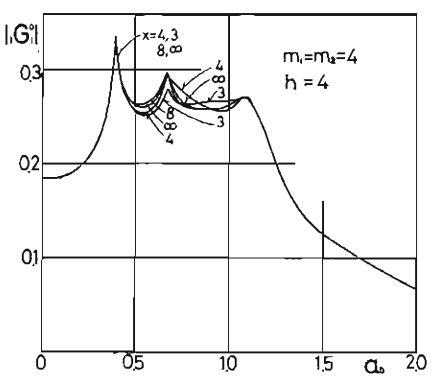

(b) $m_1=m_2=4$.

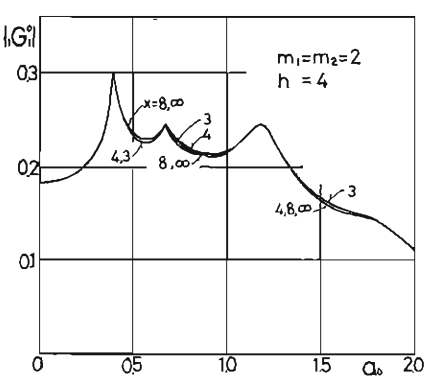

(c) $m_1=m_2=2$.

Fig. 11. Displacement amplitude characteristics of the active mass of two-mass system to force excitation, $h=4$.

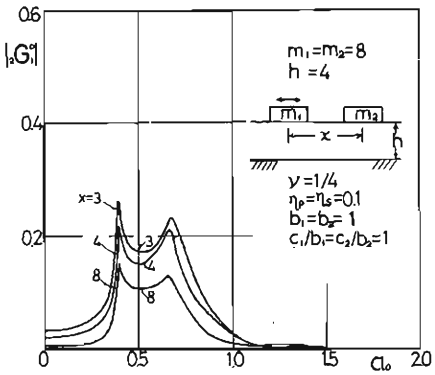

(a) $m_1=m_2=8$.

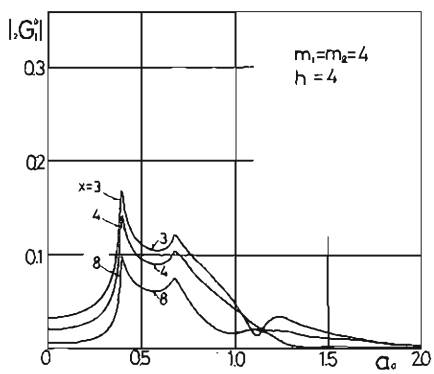

(b) $m_1=m_2=4$.

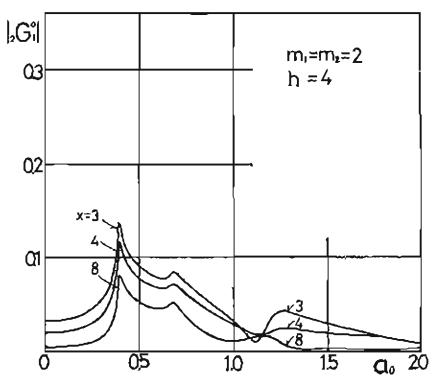

(c) $m_1=m_2=2$.

Fig. 12. Displacement amplitude characteristics of the passive mass of two-mass system to force excitation, $h=4$.

bourhood of the fundamental frequency of the stratum is significant particularly in the case where the mass ratio is small and the thickness of stratum is comparatively large, whereas when the natural frequency of the structure-subsoil system is in the lower frequency range, the lower resonance frequency with the in-phase type mode becomes important as the mass ratio is large and the distance between two masses is comparatively short as compared with the dimension of foundation. As shown in Figs. 11(a) to (c) for the case of deep stratum, there exists the resonance frequency, which seems to be inherent in the stratum, between the fundamental natural frequency of the stratum and the natural frequency of the structure-subsoil system. As the mass ratio becomes large and the lower natural frequency of the structure-subsoil system approaches to the above-mentioned resonance frequency, the second resonance becomes remarkable. From Figs. 9 to 12, it can be pointed out that the decrease of the distance between two masses does not always give monotonous effects even on the peak values of the displacement amplitude characteristics of the active mass, because the cross-interaction depends complicatedly on the exciting frequency, the dynamical characteristics and geometrical configuration of the soil-structure system, while the effects of distance on the displacement amplitude characteristics of the passive mass of the two identical masses are rather monotonous because of the preliminary filtering action by the active mass and of the rapid decay of the visco-elastic waves with the distance.

Secondly, in order to find the effects of the cross-interaction on the trasfer functions of displacements of the soil-structure system subjected to the uniform displacement excitation at the free surface of soil ground, which may be primarily concerned with the earthquake responses of structures, the multi-mass system on the visco-elastic stratum over the rigid bed rock is considered as shown in Fig. 13. Figs. 14 to 16 show the displacement amplitude characteristics $|{}_iG_S^0|$ of such a soil-structure system consisting of identical masses with the same square foundation area and equal spacing $x=4$ to the uniform displacement excitation at the free surface. Figs. 14(a) and (b) indicate comprehensively the effect of number of masses on the displacement amplitude characteristics of the soil-structure system in the cases where $h=2$ and 4, respectively.

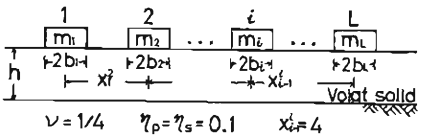

Fig. 13. *L*-mass system.

In these figures, the dotted and solid curves represent the displacement amplitude characteristics of the single mass and the two-mass system, respectively, and the broken curves show the envelope of the amplitude characteristics of each mass of the seven-mass system. From these figures it is found that when the significant resonance frequency appears in the frequency range lower than the fundamental natural frequency of the stratum, the difference between the displacement amplitude characteristics of the single mass and the two-mass systems is small for the case of the displacement excitation as compared with the case of the force excitation. This may be interpreted by the fact that the in-phase type mode of the previously-mentioned two modes is predominantly generated in the lower frequency range where the radiation damp-

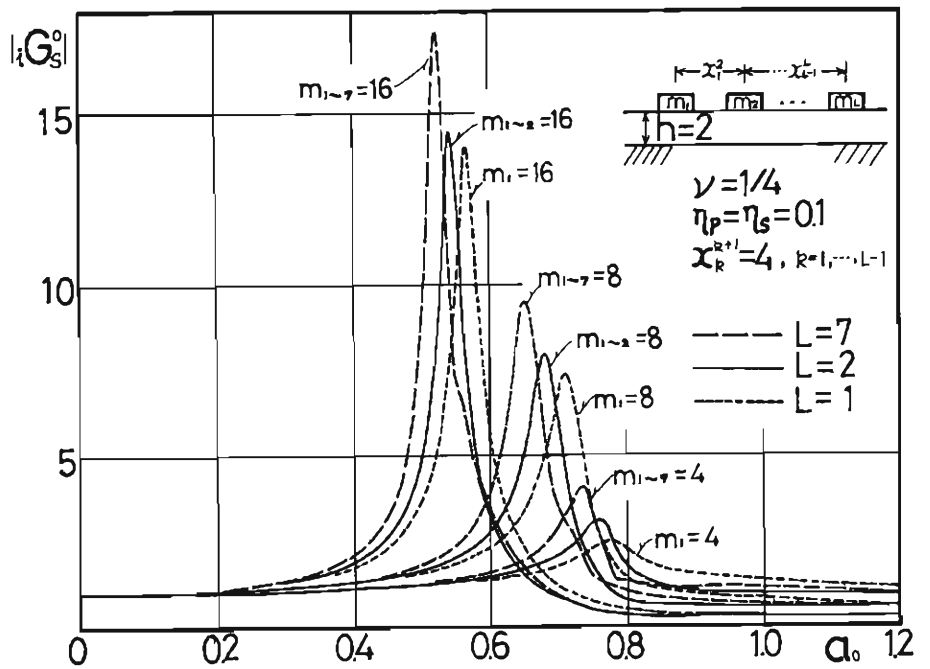

(a) $h=2$.

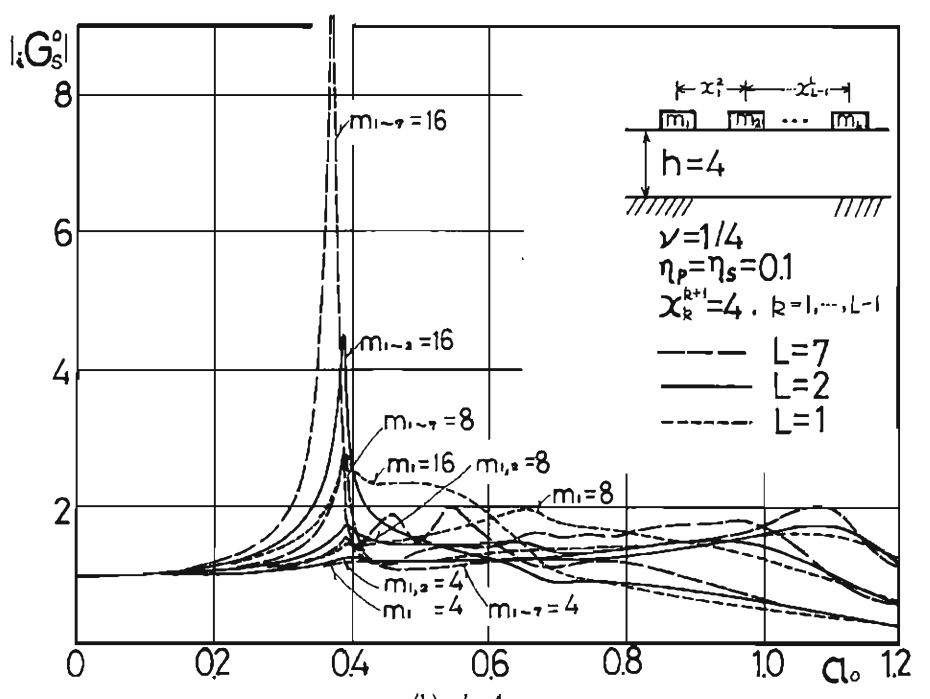

(b) $h=4$.

Fig. 14. Displacement amplitude characteristics of L-mass system to surface displacement excitation.

ing is slight, particularly for the case of identical two-mass system subjected to the uniform displacement excitation. However, when the lowest natural frequency due to the interaction between structure and its subsoil is in the frequency range higher than the fundamental natural frequency of the stratum, various modes including the above-mentioned two modes appear and their separation becomes incomplete because of the modal coupling caused by large radiation damping as well as small mass ratio. Hence, the difference between the amplitude characteristics of the two-mass system and those of the single mass system is considerably remarkable in the wide frequency range, especially in the case of deep stratum. By comparing Fig. 14(a) with Fig. 14(b), it is found that for the soil-structure system having the fundamental natural frequency within the frequency range from the fundamental natural frequency of the deep stratum to that of the shallow stratum, the peak value of the displacement amplitude characteristics of shallow stratum is remarkably larger than that of deep stratum, whereas for the soil-structure system, having the resonance frequency higher than the fundamental natural frequency of the shallow stratum, the values of the amplitude characteristics of deep stratum are somewhat larger then those of shallow stratum. In general, the value of the fundamental natural frequency of the soil-structure system decreases and the maximum peak value of the displacement amplitude characteristics increases as the number of masses of the identical multi-mass system increases. The decrease of fundamental natural frequency is simply caused by the increase of dynamic loading by masses on the surface of stratum. The increase of the maximum peak value of the displacement amplitude characteristics may be explained by two facts one of which is the dispersion of energy distribution to each mass of a multi-mass system and the other is the increase of total transmitted energy due to the degradation of damping characteristics accompanied by the increase of cross-interaction with the number of masses. Hence, as shown in Fig. 14, the effects of the number of masses are remarkable in the frequency range in which strong cross-interaction is anticipated. In the sufficiently low and high frequency ranges, the effects of the number of masses vanish irrespective to the mass ratio and the thickness of stratum. Figs. 15 and 16 show the displacement amplitude characteristics of each mass of the identical seven-mass system in the cases where $h=2$ and 4, respectively. It is found that as the mass ratio becomes large, the values of the displacement amplitude characteristics increase on the average and the dispersion about the average is large. As mentioned previously, in the case of the uniform displacement excitation, the in-phase type vibrational mode is predominantly excited at the fundamental natural frequency of the soil-structure system. In Figs. 15 and 16, it is shown that as regard to the fundamental mode the amplitude at the center-located mass is largest and it decreases considerably towards the outer masses. In the frequency range higher than the natural frequency of the stratum, the displacement amplitude characteristics are much complicated due to the complexity of ground compliance itself and of the interference among various modes. In these figures, the broken curves show the displacement amplitude characteristics of the single mass system. It is indicated that the maximum peak value of the amplitude characteristics of the seven-mass system is considerably large as compared with that of the single mass system. It is also found that there is the frequency range in which the amplitudes of the seven-mass system are smaller than the amplitude of the single mass system.

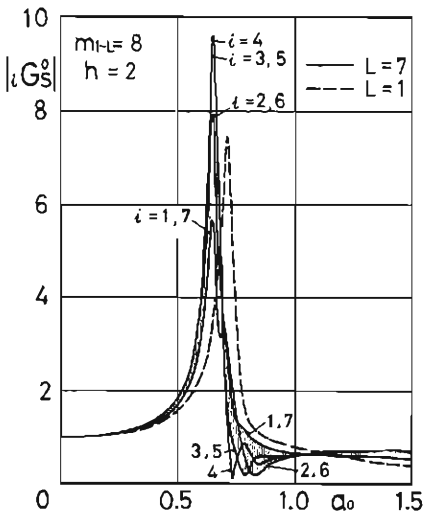

(a) $m_1 = \ldots = m_7 = 8$.

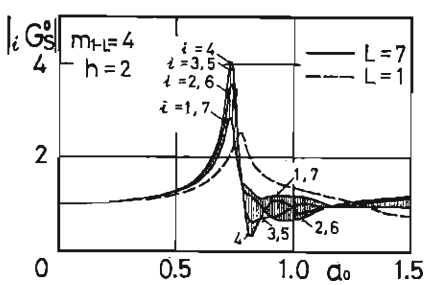

(b) $m_1 = \ldots = m_7 = 4$.

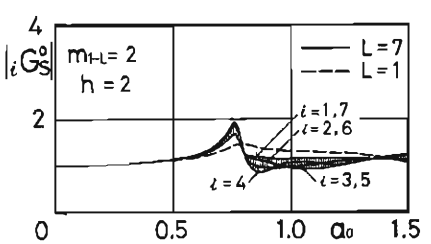

(c) $m_1 = \ldots = m_7 = 2$.

Fig. 15. Displacement amplitude characteristics of seven-mass system to surface displacement excitation, $h=2$.

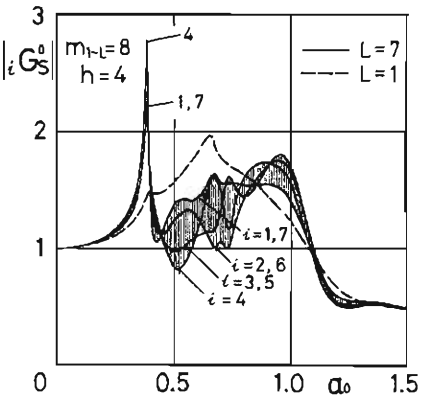

(a) $m_1 = \ldots = m_7 = 8$.

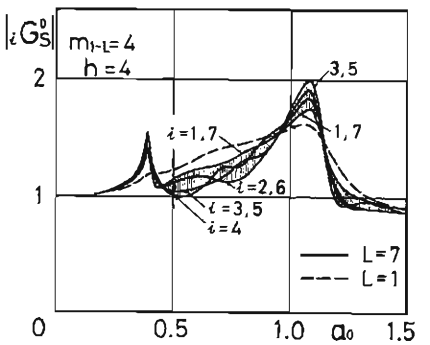

(b) $m_1 = \ldots = m_7 = 4$.

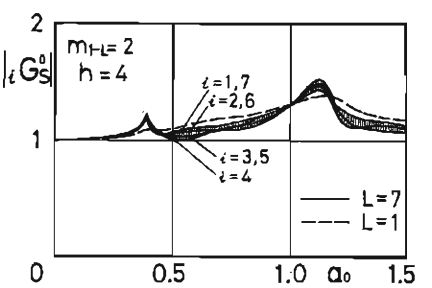

(c) $m_1 = \ldots = m_7 = 2$.

Fig. 16. Displacement amplitude characteristics of seven-mass system to surface displacement excitation, $h=4$.

Next, as a more realistic model of the soil-structure system than the model shown in Fig. 6, the dual-spring-mass system with the distance $x=4$ and the same square fundation area on the Voigt type visco-elastic stratum over the rigid bed rock is considered as shown in Fig. 17. Denoting the characteristics of the i-th structure by

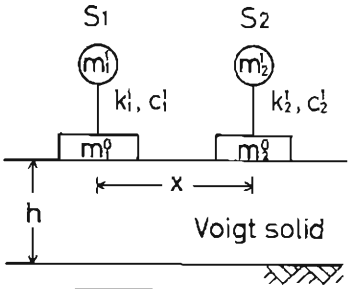

$$\lambda_i = \frac{\sqrt{k_i^1 / m_i^1}}{\pi/2h}$$

$$\zeta_i = \frac{c_i^1}{2\sqrt{m_i^1 k_i^1}}$$

S_i	$\{m_i^0, m_i^1, \lambda_i\}$
I	{1.0, 1.2, 1.5}
II	{1.0, 2.0, 1.0}
III	{1.0, 3.6, 0.6}

$\nu = 1/4$
$\eta_p = \eta_s = 0.1$
$b_1 = b_2 = 1$
$\zeta_1 = \zeta_2 = 0.01$
$x = 4$

Fig. 17. Two-spring-mass system.

$S_i=\{m_i^0, m_i^1, \lambda_i\}$, the three types of such structures are supposed, namely, $I\equiv\{1.0, 1.2, 1.5\}$, $II\equiv\{1.0, 2.0, 1.0\}$ and $III\equiv\{1.0, 3.6, 0.6\}$. Here, m_i^0 and m_i^1 denote the dimensionless masses, that is, the ratios of basement mass and upper mass of the i-th structure to the reference mass $B_0^3\rho$, respectively, and λ_i is defined as the fundamental frequency ratio of the i-th structure to the stratum, namely, $\lambda_i=(k^{i1}/m_i^1)^{1/2}/(\pi/2h)$. The values of characteristic parameters of the three structural models $S_i=I$, II and III are determined to correspond to three-story, five-story and nine-story building structures, respectively, assuming that the total mass of the upper N-story structure is given by $m_i^1=0.4N_i$ and the fundamental frequency ratio λ_i is proportional to $(N_i+1)^{-1}$, and also that the value of m_i^0 is unity for all the structural models and the value of λ_i is unity for the structural model $S_i=II$. The viscous damping coefficients of these structural models are determined by supposing the critical damping ratio $\zeta_i=0.01$ for all the models. Figs. 18 (a) and (b) show the displacement amplitude characteristics $|{}_1G_1^1|$ of the single spring-mass system to the force excitation at the basement mass in the cases where $h=2$ and 4, respectively. In these figures, the solid and broken curves correspond to the amplitude characteristics of the upper mass and those of the basement mass, respectively. It is shown that the amplitude of the basement mass decreases remarkably at the natural frequency of the structure due to the so-called dynamic absorber phemomenon and that the fundamental natural frequency of the soil-structure system appears at a slightly lower side of the natural frequency of the structure in the case of $S_i=II$ or III, whereas in

the case of $S_i=I$, it appears at a little lower side of the fundamental frequency of the stratum. When the mass ratio or the number of story becomes so large that the lowest natural frequency of the structure-subsoil system is smaller than the fundamental natural frequency of the stratum, the amplitude characteristics are sharp and their values are large because of the low damping characteristics of the lower frequency range. On the other hand, as the mass ratio or the number in story becomes small and the lowest natural frequency of the structure-subsoil system exceeds the fundamental natural frequency of the stratum, the amplitude characteristics are broadened and their values are small due to the high damping characteristics in the higher frequency range. In Figs. 18(a) and (b), it is shown that for the same value of λ_i, the peak value of the displacement amplitude characteristics of the basement mass is smaller in the case of deep stratum than in the case of shallow stratum while the peak value of the amplitude characteristics of upper mass is smaller for the shallow stratum than for deep stratum. As mentioned previously, however, for the same value of a_0 in the frequency range from the fundamental natural frequency of the deep stratum to that of the shallow stratum, the peak values of displacement amplitude characteristics of both the upper and basement masses may be larger for shallow stratum than for deep stratum. In Figs. 19(a) to (d), the displacement amplitude characteristics $|{}_1G_1^1|$ of the active spring-mass system of the identical two-spring-mass system subjected to the force excitation are shown by the solid curves for both cases where $h=2$ and 4. In these figures, broken curves represent the corresponding amplitude characteristics of the single spring-mass system. Figs. 19(a) and (c) show the amplitude characteristics $|{}_1G_1^2|$ of the upper mass while Figs. 19(b) and (d) represent those $|{}_1G_1^0|$ of the basement mass. It is indicated that the effects of the cross-interaction decrease considerably the peak value of the displacement amplitude characteristics of the active spring-mass system of the identical two-spring-mass system as compared with that of the single spring-mass system in the frequency range lower than the fundamental natural frequency of the stratum particularly in the case of $S_i=II$. However, in the frequency range higher than the fundamental natural frequency of the stratum, the amplitude characteristics are broad and the peak value of the two-spring-mass system is rather large than that of the single spring-mass system. It can be pointed out that the general features of the displacement amplitude characteristics of the identical two-spring-mass system are similar to those of the identical two-mass system, but the cross-interaction effects seem to be weaker in the former case than for the latter case for the same value of resonance frequency, especially for low resonance frequency. This may be interpreted by the fact that for the same low resonance frequency, the total mass ratio as well as the amplitude of the basement mass are much small in the case of the two-spring-mass system as compared with those of the two-mass system.

Figs. 20 (a) and (b) show the displacement amplitude characteristics $|{}_1G_s^1|$ of the single spring-mass system to the displacement excitation at the free surface of the stratum in the cases where $h=2$ and 4, respectively. The solid and broken curves indicate the amplitude characteristics $|{}_1G_s^2|$ of the upper mass and those $|{}_1G_s^0|$ of the basement mass, respectively. By comparing these figures with Figs. 18 (a) and (b), it is found that the general features of the transfer functions of the single spring-mass system to the displacement excitation are similar to those or the force excitation. In Figs. 21 (a) to (d), the displacement amplitude characteristics $|{}_1G_s^1|$ of the identical

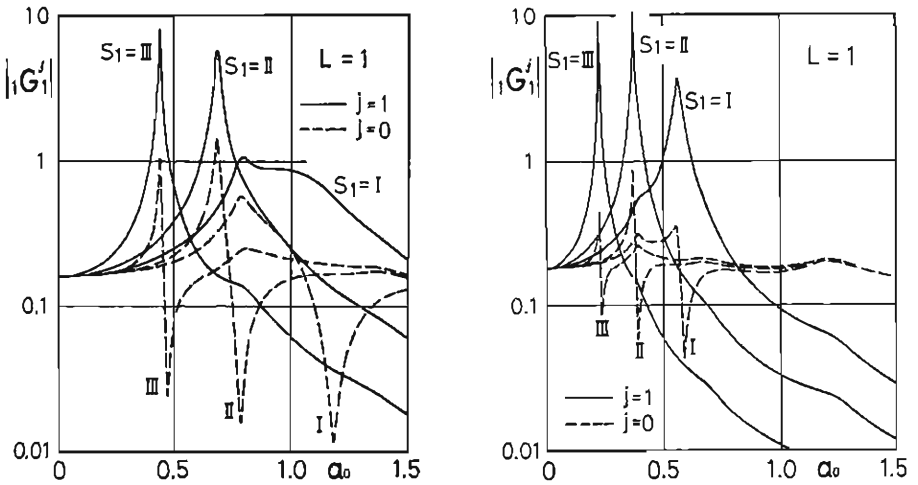

(a) $h=2$. (b) $h=4$.

Fig. 18. Displacement amplitude characteristics of single spring-mass system to force excitation.

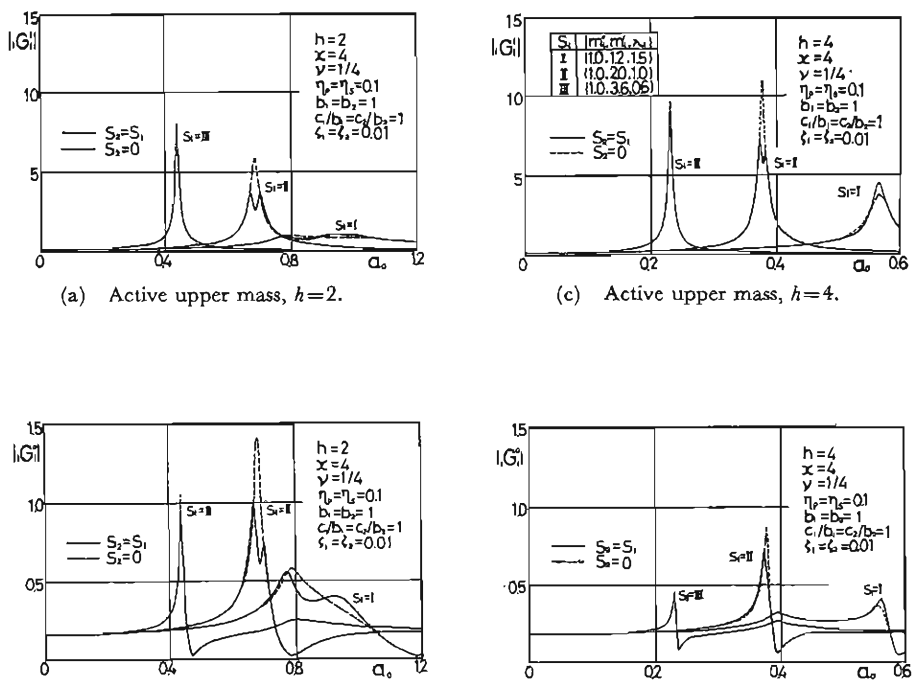

(a) Active upper mass, $h=2$. (c) Active upper mass, $h=4$.

(b) Active basement mass, $h=2$. (d) Active basement mass, $h=4$.

Fig. 19. Displacement amplitude characteristics of two-spring-mass system to force excitation.

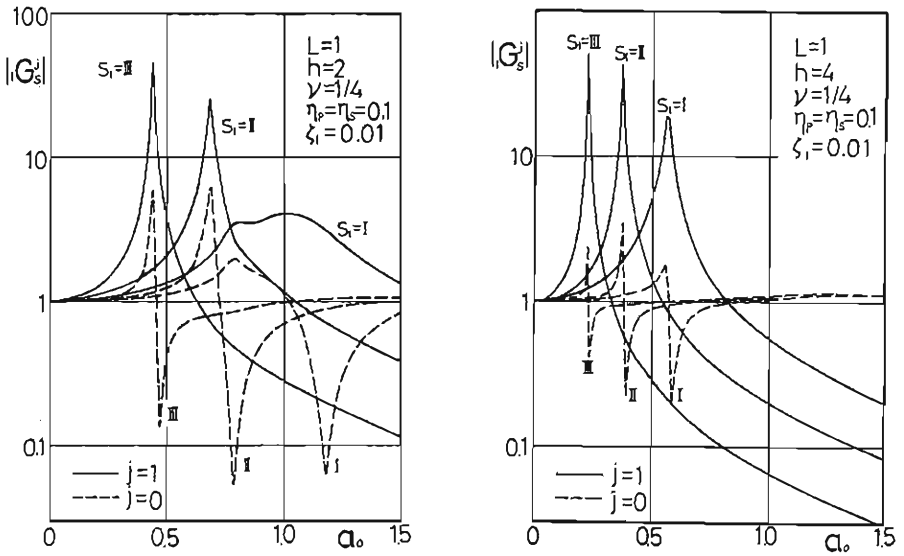

(a) $h=2$. (b) $h=4$.

Fig. 20. Displacement amplitude characteristics of single spring-mass system to surface displacement excitation.

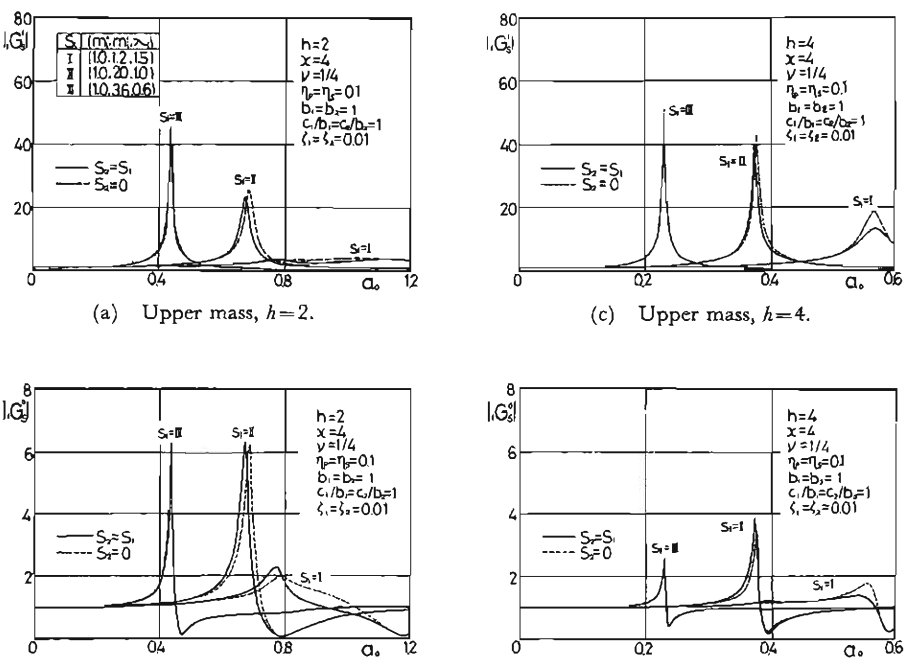

(a) Upper mass, $h=2$. (c) Upper mass, $h=4$.

(b) Basement mass, $h=2$. (d) Basement mass, $h=4$.

Fig. 21. Displacement amplitude characteristics of two-spring-mass system to surface displacement excitation.

two-spring-mass system to the uniform displacement excitation are shown for both cases where $h=2$ and 4. The broken curves in these figures represent the displacement amplitude characteristics of the corresponding single spring-mass system to the displacement excitation. By comparing Fig. 21 with Fig. 19, it can be pointed out that in the frequency range lower than the fundamental natural frequency of the stratum, the effect of the cross-interaction between the identical two-spring-mass system which decrease the peak value of the displacement amplitude characteristics to the force excitation disappears in the case of the uniform displacement excitation, whereas in the higher frequency range the cross-interaction effects seem to be the same degree for both types of excitation. These facts may be interpreted by the predominance of the in-phase type mode in the lower frequency range especially for the case of the uniform displacement excitation and by the strong modal coupling among various modes in the higher frequency range as in the case of the identical two-mass system. However, it is noted that in the higher frequency range, the peak values of the amplitude characteristics of the two-spring-mass system to the displacement excitation are smaller than those of the single spring-mass system.

Finally, to find the cross-interaction between two different structures on a viscoelastic stratum over the rigid bed rock, the displacement amplitude characteristics of two-spring-mass systems to the force excitation and those to the displacement excitation are shown in Figs. 22 and 23, respectively. In Figs. 22 (a) and (b), the displacement amplitude characteristics $|{}_1G_1^I|$ of the active spring-mass system $S_1=I$ of the different two-spring-mass system with the distance $x=4$ and to the force excitation at the active basement mass are shown, when varying the dynamical characteristics of the passive spring-mass system from $S_2=I$ to *III*. In these figures, solid and broken curves show the amplitude characteristics $|{}_1G_1^1|$ of the upper mass and those $|{}_1G_1^0|$ of the basement mass of the active spring-mass system, respectively. From Figs. 22 (a) and (b), it is found that the amplitude characteristics of the active spring-mass system are affected by the dynamical characteristics of the passive spring-mass system in the neighbourhood of the fundamental natural frequency of the passive spring-mass system. It is also found that if the dynamical characteristics, above all, the fundamental natural frequencies of the active and passive structures are close to each other, the cross-interaction effects become large even for the case where the mass ratio of the passive structure is relatively small. As for the effect of the thickness of stratum, the cross-interaction in the case of shallow stratum seems to be slightly stronger and broader as compared with the case of deep stratum. Figs. 23 (a) and (b) show the displacement amplitude characteristics $|{}_1G_S^I|$ of the spring-mass system $S_1=I$ of different two-spring-mass systems subjected to the uniform displacement excitation at the surface, when varying the dynamical characteristics S_2 of the other spring-mass system from *I* to *III* for the cases where $h=2$ and 4, respectively. In these figures, solid and broken curves represent the amplitude characteristics $|{}_1G_S^1|$ of the upper mass and those $|{}_1G_S^0|$ of basement mass, respectively. By comparing Figs. 23 (a) and (b) with Figs. 22 (a) and (b), it is found that though the general features of the displacement amplitude characteristics for both cases resemble each other, the effects of the cross-interaction in the case of the displacement excitation are stronger and broader than those in the case of the force excitation. This may be due to the fact that the displacements of both the structures are of same order in the case of the displacement excitation, whereas the displacement of the passive struc-

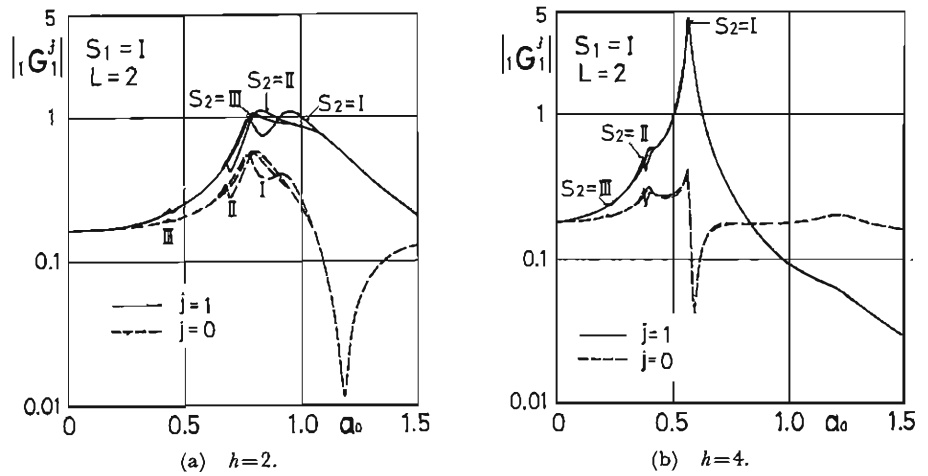

Fig. 22. Displacement amplitude characteristics of the active spring-mass system of two-spring-mass system to force excitation.

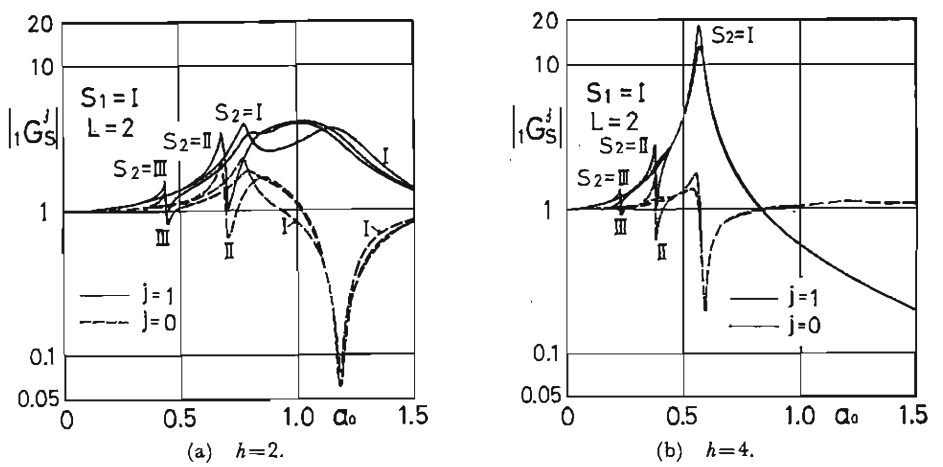

Fig. 23. Displacement amplitude characteristics of two-spring-mass system to surface displacement excitation.

ture is of lower order than that of the active structure in the case of the force excitation especially for different two structures, in other words, the cross-interaction effect in the case of the displacement excitation is primary while that in the case of the force excitation is secondary for the two structures having different dynamical characteristics. This difference of the effects of the cross-interaction between two structures on the displacement amplitude characteristics of the soil-structure system for the two types of excitation are emphasized by contrast with the resemblance between the displacement amplitude characteristics of the two types of excitation in the case of the single spring-mass system as shown in Figs. 18 and 20. From Figs. 23 (a) and (b), it is suggested that the displacement amplitude characteristics of a structure in a multi-

structure system subjected to the displacement excitation may become unexpectedly large if the adjacent structures are massive and if their fundamental natural frequencies are close to the fundamental frequency of the structure. As regard to the effects of the thickness of stratum, it is shown that the cross-interaction in the case of shallow stratum is somewhat strong as compared with the case of deep stratum, since the damping characteristics of shallow stratum are slight as compared with those of deep stratum in the frequency range from the fundamental natural frequency of deep stratum to that of shallow stratum.

Fig. 24 shows the amplitude characteristics $|G_B^S|$ of the dimensionless transfer function G_B^S of the displacement at the free surface of the stratum to the uniform displace-

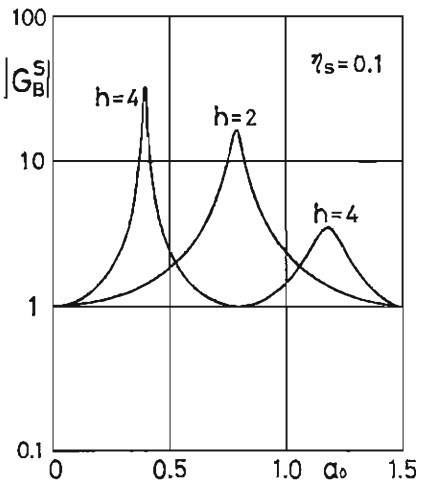

Fig. 24. Amplitude characteristics at the surface of stratum to soil-rock interface excitation.

ment excitation at the soil-rock interface in the cases where the dimensionless viscosity coefficient $\eta_s=0.1$ and the dimensionless thickness of stratum $h=2$ and 4. Simply multiplying these amplitude characteristics by the displacement amplitude characteristics of the soil-structure system to the uniform displacement excitation at the free surface, the displacement amplitude characteristics of the overall transfer functions of the soil-structure system to the uniform displacement excitation at the soil-rock interface are obtained.

4. Concluding Remarks

In order to find the effects of the cross-interaction through the soil ground on the dynamical characteristics of the multi-structure system resting on a visco-elastic stratum over the rigid bed rock, the amplitude characteristics of the dimensionless transfer functions of displacements of the soil-structure system subjected to the force excitation at one of the multi-mass system or one of the basement masses of the multi-spring-mass system and those to the uniform displacement excitation at the free surface of the stratum are numerically evaluated by varying the dynamical parameters of structures,

the number of structures, the distance between structures and the thickness of the stratum.

From these analyses, the importance of the effects of the cross-interaction on the dynamical characteristics of soil-structure systems is equally emphasized as the effects of the interaction between a structure and its surrounding subsoil ground. Though the general features of the cross-interaction effects, which are varied depending on the distribution of dynamical characteristics of structures as well as the dynamic properties of the soil ground, can not be derived from this limited analyses, some remarks arousing interest are obtained:

(1) The general trend of the dynamical characteristics and the effects of the cross-interaction on them is quite different depending on whether the lowest natural frequency due to the interaction between the structure and the surrounding subsoil is in the frequency range lower or higher than the fundamental natural frequency of the stratum. When the lowest natural frequency of the structure-subsoil system is in the lower frequency range, it becomes the fundamental natural frequency of the whole soil-structure system, and the displacement amplitude characteristics of the soil-structure system become sharp and high in the vicinity of the fundamental natural frequency due to the low damping characteristics in the lower frequency range. Hence the effects of the cross-interaction of such a soil-structure system on the dynamical characteristics of a structure included in the system appear remarkably in the vicinity of the natural frequencies contained in the lower frequency range, particularly for the case where the masses of adjacent structures are large and the dynamical characteristics of structures composing the multi-structure system are close to each other. However, in the exceptional case of the identical two structures subjected to the uniform displacement excitation, the cross-interaction effects become trivial because the in-phase mode associated with the fundamental natural frequency is predominantly excited in such case. If the lowest natural frequency of the structure-subsoil system is in the higher frequency range, on the other hand, the fundamental natural frequency of the soil-structure system is in the neighbourhood of the fundamental natural frequency of the stratum, and the displacement amplitude characteristics are broadened and their peak values are relatively small due to the high damping characteristics as well as the modal coupling among various modes. Hence the cross-interaction effects of such soil-structural system seem to be rather weak in the higher frequency range. However, the peak values of the multi-structure system are sometimes larger than those of the single structure system in such case.

(2) The effects of the cross-interaction between the identical two-structure system are different depending on the type of excitation as well as the relative location of the lowest natural frequency of the structure-subsoil system to the fundamental natural frequency of the stratum. If the lowest natural frequency of the structure-subsoil system is in the lower frequency range, and if it is the case of force excitation, the cross-interaction effects act to decrease considerably the peak value of displacement amplitude characteristics due to interference between two modes, one of which is in-phase type and the other is out-of-phase type. As mentioned previously, however, in the case of uniform displacement excitation, the effects of cross-interaction are small due to predominance of the in-phase type mode. On the other hand, when the lowest natural frequency of the structure-subsoil system is in the higher frequency range, the dynamical characteristics of the soil-structure system are influenced by the cross-

interaction in the wide frequency range including the lower natural frequencies of the system. However, the difference of the cross-interaction effects is not distinct for the two types of excitation.

(3) As the number of identical structures increases, the cross-interaction effects become strong even in the case of the uniform displacement excitation at the free surface of the stratum. Since the various modes produced by the coupling between the multiple structures and the stratum make the displacement characteristics of each structure spread and since the dynamic loading by a large number of masses on the surface of the stratum makes the transmitted energy due to displacement excitation to the multi-structure system increase, the maximum peak value of the displacement amplitude characteristics of the structures becomes considerably large.

(4) The effects of the cross-interaction between the two structures having different dynamical characteristics on the displacement amplitude characteristics of one of the structures appear in the vicinity of the fundamental natural frequency of the other structure. In general, such interaction effects are remarkable if the mass ratio of the latter structure is relatively large and if the dynamical characteristics are not so different from each other. Also, the effects of the cross-interaction between structures are more significant in the case of displacement excitation than for force excitation because the cross-interaction is primary in the former case and secondary in the latter case.

(5) The effects of the thickness of stratum on the cross-interaction may be small when the lowest natural frequency of the structure-subsoil system is sufficiently small or large as compared with the fundamental natural frequency of the stratum. If the lowest natural frequency of the structure-subsoil system is in the intermediate frequency range containing the fundamental natural frequency of the stratum, the cross-interaction effects of the soil-structure system are complicatedly influenced by the thickness of stratum. In the case of shallow stratum, the fundamental natural frequency of the soil-structure system is likely to be of the structure-subsoil resonance type. On the other hand, in the case of deep stratum, the fundamental natural frequency is of the stratum resonance type. Hence, for the soil-structure system having the fundamental natural frequency within the frequency range from the fundamental natural frequency of the deep stratum to the shallow stratum, the peak value of the displacement amplitude characteristics of shallow stratum is larger than that of deep stratum. However, in the frequency range higher than the fundamental natural frequency of the shallow stratum, the peak values of deep stratum are somewhat large as compared with those of shallow stratum. Similar discussions as mentioned above can be adapted for the effects of the thickness of stratum on the cross-interaction.

From the above-mentioned remarks, it is evident that in doing the aseismic design of a structure, the effects of the cross-interaction between the structure and adjacent structures through soil ground together with the effects of dynamic loading of structures over the surface of the soil ground should be taken into consideration besides the interaction between the structure and its surrounding subsoil and the filtering action of the soil layers, particularly in the big cities having high density of structures on a soft soil ground. In estimating the effects of the cross-interaction, it may be important to know the relation between the fundamental natural frequency of the soil-structure system and that of the soil layers, the distribution of dynamic loading

over the soil layers at the present as well as in the future, and especially the relation between the fundamental frequency of the structure to be designed and those of adjacent structures.

Acknowledgement

All numerical computations in this paper were made with the aid of the digital computer FACOM 230–60 at the Data Processing Center of Kyoto University.

References

1) Bycroft, G. N.: Forced Vibrations of a Rigid Circular Plate on a Semi-Infinite Elastic Space and on an Elastic Stratum, Philosophical Transaction of the Royal Society of London, Vol. 248, Series A, 1956, pp. 327–368.
2) Kobori, T.: Dynamical Response of Rectangular Foundations on an Elastic-Space, Proceedings of Japan National Symposium on Earthquake Engineering, 1962, pp. 81–86.
3) Thomson, W. T. and T. Kobori: Dynamical Compliance of Rectangular Foundations on an Elastic Half-Space, Journal of Applied Mechanics, Vol. 30, Series E, No. 4, 1963, pp. 579–584.
4) Kobori, T., R. Minai, T. Suzuki and K. Kusakabe: Dynamical Ground Compliance of Rectangular Foundation on a Semi-Infinite Elastic Medium, Annuals of the Disaster Prevention Research Institute, Kyoto University, No. 10A, 1967, pp. 283–314 (in Japanese).
5) Kobori, T., R. Minai, T. Suzuki and K. Kusakabe: Dynamical Ground Compliance of Rectangular Foundation, Proceedings of the Sixteenth Japan National Congress for Applied Mechanics, 1967, pp. 301–306.
6) Kobori, T., R. Minai and T. Suzuki: Dynamical Ground Compliance of Rectangular Foundation on an Elastic Stratum over a Semi-Infinite Rigid Medium, Annuals of the Disaster Prevention Research Institute, Kyoto University, No. 10A, 1967, pp. 315–341 (in Japanese).
7) Kobori, T., R. Minai and T. Suzuki: Dynamical Ground Compliance of Rectangular Foundation on an Elastic Stratum over a Semi-Infinite Rigid Medium (Continued), Annuals of the Disaster Prevention Research Institute, Kyoto University, No. 11A, 1968, pp. 331–347 (in Japanese).
8) Kobori, T., R. Minai, T. Suzuki and K. Kusakabe: Dynamical Ground Compliance of Rectangular Foundation on a Semi-Infinite Visco-Elastic Medium, Annuals of the Disaster Prevention Research Institute, Kyoto University, No. 11A, 1968, pp. 349–367 (in Japanese).
9) Kobori, T., R. Minai, T. Suzuki and K. Kusakabe: Vibrational Characteristics of Semi-Infinite Visco-Elastic Medium to Surface Excitations on a Rectangular Area, Annuals of the Disaster Prevention Research Institute, Kyoto University, No. 12A, 1969, pp. 301–316 (in Japanese).
10) Kobori, T., R. Minai and K. Kusakabe: Vibrational Characteristics of Semi-Infinite Visco-Elastic Medium to Surface Excitations on a Rectangular Area (Part 2), Annuals of the Disaster Prevention Research Institute, Kyoto University, No. 13A, 1970, pp. 233–250 (in Japanese).
11) Kobori, T., R. Minai and K. Kusakabe: Vibrational Characteristics of Semi-Infinite Visco-Elastic Medium to Surface Excitations on a Rectangular Area (Part 3), Annuals of the Disaster Prevention Research Institute, Kyoto University, No. 14A, 1971, pp. 253–262 (in Japanese).
12) Kobori, T., R. Minai and T. Suzuki: The Dynamical Ground Compliance of a Rectangular Foundation on a Viscoelastic Stratum, Bulletin of the Disaster Prevention Research Institute, Kyoto University, Vol. 20, Part 4, March, 1971, pp. 289–329.
13) Kobori, T., R. Minai and T. Suzuki: Dynamical Characteristics of Structures on an Elastic

Ground, Annuals of the Disaster Prevention Research Institute, Kyoto University, No. 9, 1966, pp. 193–224 (in Japanese).

14) Kobori, T., R. Minai, T. Suzuki and K. Kusakabe: Dynamical Characteristics of Structure of Rectangular Foundation, Proceedings of Japan Earthquake Engineering Symposium-1966, 1966, pp. 273–278 (in Japanese).

15) MacCalden, P. B.: Transmission of Steady-State Vibrations between Rigid Circular Foundations, Ph. D. Thesis, Univ. of Calif., Los Angeles, 1969.

16) Warburton, G. B., J. D. Richardson and J. J. Webster: Forced Vibrations of Two Masses on an Elastic Half-Space, Journal of Appl. Mech. Vol. 37, No. 1, 1971, pp. 148–156.

17) Kobori, T., R. Minai and K. Kusakabe: Vibrational Characteristics of a Coupled Rigid Bodies System on an Elastic Ground, Reports of the Architectural Institute of Japan (Kinki Sub-Division), 1971, pp. 13–16 (in Japanese).

18) Kobori, T.: Random Vibrations of Structure-Foundation Interaction System, Proc. of the 3rd U. S. – Japan Joint Seminar on Stochastic Methods in Dynamical Problems, 1971.

19) Kobori, T. and R. Minai: One-Dimensional Wave-Transfer Functions of the Linear Visco-Elastic Multi-Layered Half-Space, Bulletin of the Disaster Prevention Research Institute, Kyoto University, Vol. 18, Part 4, March, 1969, pp. 27–64.

20) Kobori, T., R. Minai and T. Suzuki: Wave Transfer Functions of Inhomogeneous Linear Viscoelastic Multi-Layered Media, Annuals of the Disaster Prevention Research Institute, Kyoto University, No. 13A, 1970, pp. 213–232 (in Japanese).